# Fast Simulation of Electromagnetic Showers in a Homogeneous Crystal Calorimeter

I. Phys. Institute, RWTH Aachen

July 6, 1993

(H. Hillemanns, W. Krenz, and D. Schmitz)

Abstract

We investigate the fast simulation of electromagnetic showers in homogeneous detector arrays. The study is based on a program, developed for the uranium-scintillator sampling calorimeter of the ZEUS experiment and is equally well suited for homogeneous detectors.

In our report we use electrons as incident particles, but – with small modifications – the program can also be used for photons. We describe the application of the method to different calorimeter setups (different volumes) and various materials ($CeF_3$, $PbF_2$ and $BaF_2$). Longitudinal and radial shower profiles as well as energy and space resolutions were studied.

The Program uses parametrizations for the longitudinal and radial shower profiles, where the latter ones depend on the depth in the material. For the most important parameters approximate relations (of the order of 10 %) depending on the radiation length and the Moliere radius of the material are given.

Fluctuations are taken into account by randomly varying the locations of energy deposition, resulting in a fluctuation of the energy deposited in the detector volume, and by fluctuating appropriate shower shape parameters. For our studies the fast Monte-Carlo program was roughly 100 times faster than the corresponding EGS4/GEANT simulation.

# 1 Introduction

Monte-Carlo studies for data analysis and future detector design for high energy experiments at LHC, SSC or similar accelerators will take an enormous amount of computer time. Both, the very detailed simulation of electromagnetic showers with EGS4/GEANT [1] and the hadronic shower development will be extreamly time consuming. In this report we investigate the simulation of electromagnetic shower development by a parametrized Monte-Carlo Program. Showers induced by electrons will be considered only.

The time spent for a detailed detector simulation of an electron or photon is approximately proportional to the energy of the showering particle. This comes from the fact that the electron-photon cascade has to be simulated down to rather low energies. One might remember that about 40 % of the energy deposition of a 10 GeV electron comes from electrons and photons below 1 MeV. Therefore, a detailed study of the response of an inhomogeneous detector with e.g. layers of different materials in a complicated geometry or blind regions requires full EGS/GEANT simulation.

On the other hand, to answer with sufficient accuracy various questions on shower development – e. g. on longitudinal and transverse shower profiles, on energy containment, on estimates for energy resolution, or on spatial and angular resolution – it might be worthed to investigate a fast Monte-Carlo simulation (FMC) based on parametrized shower profiles. Also the problem of trigger efficiency and acceptance might be solved with a FMC. Naturally, such programs can only describe the global behaviour of showers. Details connected for instance with individual electromagnetic processes and energy deposits related to them remain hidden.

The quality of such studies will of course depend on the quality of shower parametrization. For the longitudinal shower development there exists a well known parametrization by Longo and Sestili quoted in the Review of Particle Properties [3]. The parametrization of the transverse profile is not determined with the same precision. It will be seen that for the radial parametrization essentially the same expression as for the longitudinal part was used with a slight modification in the exponential term.

We followed the description of a FMC by del Peso and Ros for the ZEUS calorimeter [2] and applied it to homogeneous calorimeters of different sizes and various materials. This program was preferred, since specially the simulation of the radial shower profiles is treated more rigorously than in previous fast simulation programs.

The program depends on a complete set of 17 parameters which have carefully to be adjusted to the special detector under study. The fine tuning of all parameters is rather tedious, but it increases the predictive power of the program. Therefore the FMC should be mainly used for existing detectors or new ones, where the design is finished. For studies of detector designs with different geometrical structures and/or varying materials one might run with a reduced accuracy and therefore does not need fine tuning of the parameters.

In this report we give in chapter 2 a short description of the simulation method, specifying the longitudinal and radial shower parametrizations and making some remarks on shower fluctuations. Chapter 3 explicitely gives the most relevant parameters for $CeF_3$, $PbF_2$ and $BaF_2$ and shows their energy dependence. For these parameters and their fluctuations we derive approximate parametrizations depending on the radiation length and the Moliere radius of the material. A comparison between FMC and GEANT (version 3.14) simulation is performed in chapter 4. Here longitudinal and radial shower profiles generated with the FMC program are compared to GEANT predictions. In chapter 5 we show for 10 GeV electrons the energy and space resolution in a homogeneous crystal matrix consisting of $CeF_3$ as a function of the size

of the detector.

# 2 Short Description of the Simulation Method

## 2.1 General Determination of Shower Shape Parameters

Longitudinal and radial energy distributions of electron showers, generated with EGS4/GEANT, serve to find the best set of parameters for the FMC program. The goal is to achieve the best agreement between simulated GEANT and FMC shower profiles for a reasonable energy range (e.g. 2 to 100 GeV). The distributions produced by GEANT depend on the electron and photon cut-off parameters. Very low cut-off parameters allow very accurate simulations down to detailed processes of very low energy electrons and photons, but are extremely time consuming. For our calculations we assigned cut-off energies of 1.5 MeV for electrons and 100 keV for photons. We used the GEANT program (version 3.14) to generate in $CeF_3$ some hundred electron showers at six different energies (2, 5, 10, 20, 50 and 100 GeV); in $BaF_2$ and $PbF_2$ at each of three energies (5, 10 and 50 GeV) only 100 events were generated. An increase of statistics does not change the results significantly.

The meaning and the determination of the shower shape parameters is described in the following subsections. Only a short description will be given here; for any details we refer to the above mentioned DESY-report.

## 2.2 Longitudinal Profile

The longitudinal shower profile is based on a formula for energy deposition given in the Review of Particle Properties [3]. It is assumed that an electron with energy $E$ moves in $z$-direction and hits a material at $z = 0$ perpendicular to the front face. Denoting the depth in the material by $l = z/X_0, X_0$ being the radiation length, the energy deposition has the form:

$$\frac{1}{E}\frac{dE}{dl} = \frac{b_z(b_z l)^{\alpha_z - 1} e^{-b_z l}}{\Gamma(\alpha_z)} \tag{1}$$

With the alternative parameter $\lambda_z = X_0/b_z$ this relation was rewritten [2] :

$$f_L(z) = \frac{1}{E}\frac{dE}{dz} = \left(\frac{z}{\lambda_z}\right)^{\alpha_z - 1} \cdot \frac{e^{-z/\lambda_z}}{\lambda z \cdot \Gamma(\alpha_z)} \tag{2}$$

This distribution is normalized to one:

$$\int_0^\infty f_L(z)dz = 1$$

In principle one could fit this formula to average longitudinal shower profiles and derive the parameters and their fluctuations. However, in the fitting procedure gaussian distributed parameters are assumed, which in reality are non-gaussian. It was shown by Grindhammer et al. [4] that for an adequate treatment of non-gaussian parameter fluctuations one should use moments with respect to the z-coordinate of the energy distribution to receive reliable information on both, parameters and their fluctuations. The n-th moment for the longitudinal distribution is given by:

$$Z_n = \int_0^\infty z^n f_L(z)dz = \lambda_z^n \frac{\Gamma(\alpha_z + n)}{\Gamma(\alpha_z)} \tag{3}$$

Particularly:

$$Z_1 = \alpha_z \cdot \lambda_z \quad \text{and} \quad Z_2 = \lambda_z^2 \cdot \alpha_z(\alpha_z + 1) \tag{4}$$

Solving these equations for the parameters one receives:

$$\alpha_z = \frac{Z_1^2}{Z_2 - Z_1^2} \quad \text{and} \quad \lambda_z = \frac{Z_2 - Z_1^2}{Z_1} \tag{5}$$

During the simulations of the reference samples with GEANT for each event the moments $Z_1$ and $Z_2$ and from those the parameters $\alpha_z$ and $\lambda_z$ were calculated. In chapter 3 we will display histograms of these parameters showing their average values and their fluctuations.

## 2.3 Radial Profile

If $r$ denotes the radial distance from the shower axis the radial energy distribution function - analogous to the longitudinal one (2) - is given by:

$$f_T(z,r) = \frac{1}{2} \cdot \left(\frac{r}{\lambda_r}\right)^{\frac{\alpha_r}{2}-1} \cdot \frac{e^{-\sqrt{r/\lambda_r}}}{\lambda_r \Gamma(\alpha_r)} \tag{6}$$

Again - for each value of z - this distribution is normalized to one:

$$\int_0^\infty f_T(z,r)dr = 1$$

The parameter $\alpha_r$ in equ. (6) depends on the depth in the material and can approximately be written in the form $\alpha_r = 0.5 + \alpha_r' \cdot z$. This results from a fit of the distribution function (6) to the GEANT radial distributions at different shower depths.

No analytic expression can be given for the pure radial part of the distribution:

$$f_T(r) = \int_0^\infty f_T(z,r) \cdot f_L(z)dz \tag{7}$$

As for logitudinal distributions the moments can be used to extract the parameters $\alpha_r'$ and $\lambda_r$ from GEANT data. In general the $n^{th}$ moment is written:

$$\begin{aligned} R_n &= \int_0^\infty r^n f_T(r)dr \\ &= \int_0^\infty f_L(z)dz \cdot \lambda_r^n \frac{\Gamma(\alpha_r + 2n)}{\Gamma(\alpha_r)} \end{aligned} \tag{8}$$

In particular one calculates:

$$R_{1/2} = \sqrt{\lambda_r} \cdot (0.5 + \alpha_r' Z_1) \tag{9}$$

$$R_1 = \lambda_r \cdot (0.75 + 2\alpha_r' Z_1 + \alpha_r'^2 Z_2) \tag{10}$$

These equations can be solved for the parameters $\alpha_r'$ and $\lambda_r$, leading to:

$$\alpha_r' = -\frac{(\epsilon_r - 2)Z_1}{2(\epsilon_r Z_1^2 - Z_2)} + \frac{1}{2(\epsilon_r Z_1^2 - Z_2)} \cdot \sqrt{Z_1^2(4 - \epsilon_r) - Z_2(3 - \epsilon_r)} \tag{11}$$

$$\lambda_r = \frac{R_{1/2}^2}{(0.5 + \alpha_r' Z_1)^2} \tag{12}$$

where $\epsilon_r = R_1 / R_{1/2}^2$.

## 2.4 Remark on Shower Fluctuations

In the FMC program the total energy ($E_0$) of the incident electron is distributed equally over $N(E_0)$ hits. The locations of the hits are randomly chosen from the distribution functions (2) and (6). In general, there are two indepentent contributions to fluctuations which also independently influence FMC predictions on energy or space resolution:

- Intrinsic fluctuation ($\sigma_i$) are related to global shower fluctuations. They are simulated by fluctuating the parameters $\alpha_z$ and $\lambda_z$ of the longitudinal distribution and $\alpha'_r$ and $\lambda_r$ of the radial distribution around their mean values.

- Sampling fluctuations (or statistical fluctuations $\sigma_s$) lead to local shower fluctuations. These are simulated by fluctuating the position of the energy deposition, i. e. the position of the hit in the FMC. Local shower fluctuations are proportional to $1/\sqrt{N}$; therefore an infinite number of hits inside the detector reproduces the shower profiles exactly. For sampling calorimeters the statistical fluctuations contribute a term $b/\sqrt{E}$ to the energy resolution, where $b$ depends on details of the detector setup. For homogeneous detectors the energy resolution might differ from the $1/\sqrt{E}$ rule due to many effects, e. g. noise, pedestal fluctuations, nonuniformities of light collection, calibration errors. To match the energy resolution of the calorimeter, as simulated by GEANT, the number of hits in the FMC is an extremely important parameter. It has to be tuned for each special detector under study (ch. 5).

# 3 Parameters for $CeF_3$, $BaF_2$ and $PbF_2$

In general for FMC shower simulation the energy $E_0$ of the incident electron and 17 parameters are needed; these are:

- Number of hits, $N(E_0)$;

- Four shower shape parameters, two for the longitudinal ($\alpha_z$ and $\lambda_z$) and two for the radial energy distribution ($\alpha'_r$ and $\lambda_r$). Actually the logarithms are used as explained below;

- Four Standard Deviations of these logarithmic parameters;

- Two parameters for the deformation of the transverse shower profile;

- Six correlation parameters (see DESY-report for details).

These parameters have to be optimized in such a way that FMC and GEANT results show a fair agreement. The technique for doing this is described in detail in the DESY-report and will not be repeated here.

The parameters discussed in this section are the shape parameters and their fluctuations needed to describe the longitudinal and radial shower profiles. Figs. 1 a-d show the distributions of the parameters $\alpha_z$, $\lambda_z$ and $\alpha'_r$, $\lambda_r$ for 10 GeV electrons incident on $CeF_3$. They were determined for each event from the respective moments as described above. It is recognized that these parameters – except possibly $\lambda_r$ – are not gaussian distributed. Somewhat more gaussian-like distributions are shown in fig. 2, where the logarithms of the four parameters are displayed. This seems to be a general behaviour of the parameters and is also true for different energies and materials. Therefore the mean values and Standard Deviations used in the FMC

have been determined from gaussian fits to distributions of the logarithms of the parameters. Fig. 3 shows the logarithms of the four parameters for $CeF_3$ as a function of the incident electron energy. All parameters (p) depend linearly on the logarithm of the energy and can be parametrized in the form $ln\ p = a + b \cdot ln\ E$. The curves in fig. 3 are fits of this parametrization to the Monte-Carlo data.

The longitudinal (radial) development of an electromagnetic shower in different materials scales fairly accurately with the radiation lenght (Moliere radius) of the respective material. From an investigation of three materials ($CeF_3$, $BaF_2$ and $PbF_2$) at different energies (5, 10 and 50 GeV) we were able to derive approximate parametrizations for the above mentioned parameters, provided that radiation length ($X_0$) and Moliere radius ($R_M$) of the materials are known. $X_0$ has been measured for many detector materials and different approaches lead to almost identical results. We have used the algorithm described in the GEANT manual. In contrast the values for the Moliere radii are widely spread depending on the procedure to derive it. We used the relation:

$$R_M = \frac{21.2\ MeV}{E_c} \cdot X_0 \tag{13}$$

where $E_c$ is the critical energy of the showering particle (electron). At the critical energy the particle looses the same amount of energy through ionization and radiation (bremsstrahlung). For our study the critical energy was calculated by [3]:

$$E_c = \frac{800\ MeV}{Z_{eff} + 1.2} \tag{14}$$

These relations lead to Moliere radii which are somewhat larger compared to the more exact calculations following the 'Review of Particle Properties [3]', but they are in many cases much smaller than values given in the literature (produced mainly by GEANT with the prescription: 90 % of the energy is contained in a cylinder of radius 1 $R_M$, 95 % in 2 $R_M$ and 99.5 % in 3 $R_M$, see also [3]). The values actually used are given in table 1. For a parametrization depending only on radiation length and Moliere radius of a material equ. (1) is used for the longitudinal profile and equ. (6) is rewritten in a different form. For convenience, we repeate equ. (1):

Longitudinal Profile

$$\frac{1}{E}\frac{dE}{dl} = \frac{b_z(b_z l)^{\alpha_z - 1} e^{-b_z l}}{\Gamma(\alpha_z)} \tag{15}$$

where $l = z/X_0$ and $b_z = X_0/\lambda_z$.

Radial Profile

$$\frac{1}{E}\frac{dE}{dt} = \frac{1}{2}\frac{b_r(b_r t)^{\frac{\alpha_r}{2} - 1} e^{-\sqrt{b_r t}}}{\Gamma(\alpha_r)} \tag{16}$$

where $t = r/R_M$, $b_r = R_M/\lambda_r$ and $\alpha_r = 0.5 + \alpha'_r \cdot z$.

The parametrizations are then as follows ($E$ in $GeV$):

$$ln\ \alpha_z = 1.062 + 0.129 \cdot ln\ E \tag{17}$$

$$b_z = 0.483 + 0.009 \cdot ln\ E \tag{18}$$

$$ln\ \alpha'_r = -0.840 \cdot X_0 - 0.190 \cdot ln\ E \tag{19}$$

$$b_r = 20.36 - 1.860 \cdot ln\ E \tag{20}$$

Table 1: Radiation length and Moliere radius (in $cm$)

| Material | $X_0$ | $R_M$ |
|---|---|---|
| $PbF_2$ | 0.94 | 1.8 |
| $BaF_2$ | 2.03 | 2.5 |
| $CeF_3$ | 1.66 | 2.0 |

Table 2: Parameters for $\sigma_{ln\ p_i}(E)$

| $p_i$ | a | b | c | d |
|---|---|---|---|---|
| $\alpha_z$ | 0.080 | 0.700 | 0.266 | 3.000 |
| $\lambda_z$ | 0.060 | 2.360 | 1.500 | 3.000 |
| $\alpha'_r$ | 0.157 | 2.070 | 0.100 | 4.140 |
| $\lambda_r$ | 0.050 | 2.400 | 0.300 | 3.500 |

The energy dependent values of the logarithms of the parameters ($ln(\alpha_z)$, $ln(\lambda_z)$, $ln(\alpha'_r)$, and $ln(\lambda_r)$) and the curves corresponding to the approximations (eqns. 17 - 20) are shown in figs. 4, 5 and 6 for $CeF_3$, $BaF_2$ and $PbF_2$, respectively. The parametrizations agree reasonably well with all data sets.

The z-dependence of $\alpha_r$ (see ch. 2.3) can be written in the general form:

$$\alpha_r(z) = 0.5 + \frac{0.270}{R_M} \cdot z \tag{21}$$

For 10 GeV electrons figs. 7 and 8 display $\alpha_r(z)$ for $CeF_3$ and $BaF_2$, respectively. The points are determined with GEANT, whereas the parametrization (21) is shown as full line. The agreement is good.

Also the standard deviations of the logarithms of the parameters are parametrized. Since the Monte-Carlo calculations do not depend very sensitively on the exact $\sigma$'s, the approximations are rather crude. The parametrization is written in the form ($E$ in $GeV$):

$$\sigma_{ln\ p_i}(E) = a + \frac{b}{(ln\ E + c)^d} \tag{22}$$

Fig. 9 shows the Standard Deviations of the logarithms of the parameters, the curves are fits using relation (22). As expected the fluctuations decrease with increasing energy, the strongest decrease being in the Standard Deviations of the radial parameters. Table 2 contains the parameters a, b, c, and d as determined in the fits.

# 4 FMC-GEANT-Comparison

## 4.1 Longitudinal and Radial Profiles

As an example we show in figs. 10 a, b the longitudinal (equ.2) and radial shower profiles (equ. 6) for a 10 GeV electron in $CeF_3$, where the full lines correspond to the equations and the histograms result from EGS/GEANT events. The radial distribution was taken at a depth of 15 cm ($\sim$ 7.5 $X_0$). For both energy distributions the agreement between GEANT and parametrized functions are reasonable; at distances larger than 8 cm ($\approx$ 4 $R_M$ !) from the shower axis the parametrization is somewhat too low. One should, however, remember that about 99.5 % of the energy deposited in the detector lies within 3 Moliere radii!

Figs. 11 and 12 compare the longitudinal shower profiles for FMC and GEANT simulations for 10 and 50 GeV electrons in $CeF_3$. The percentage of energy deposited is plotted as a function of $z$, the depth in the material. The histogram results from GEANT, the dots from FMC simulation. The overall agreement is reasonable. The peaks occur about in the same depths ($z = 10cm$ and $z = 13cm$, respectively) and the overall shapes are identical.

For 10 GeV electrons the same comparison is shown for $BaF_2$ and $PbF_2$ in figs. 13 and 14, respectively. In both cases the agreement between GEANT and FMC is good.

Fig. 15 shows a FMC/GEANT comparison of the mean values of the shower depth in $CeF_3$ (that is the first longitudinal moment $Z_1$, eqn. 4) as a function of the incident electron energy. The agreement is perfect for all energies.

Figs. 16 and 17 show the z-integrated radial shower profiles for 10 and 50 GeV electrons incident on $CeF_3$. For both energies the agreement between FMC and GEANT simulation is satisfactory; as mentioned above there are slight deviations beyond about 3 Moliere radii where the energy deposition is fairly small. Figs. 18 and 19 compare radial shower profiles from GEANT and FMC for 10 GeV electrons in $BaF_2$ and $PbF_2$, respectively.

## 4.2 Radial Profiles as Function of Depth

The development of an electromagnetic shower shows always – independent of the material – the same characteristic structure. It starts with a single electron (or an $e^+e^-$-pair in case of an incident photon) which leads within the first few radiation lenghts to a narrow region of energy deposition (a central core) surrounded by a halo. After about 5 to 7 radiation lengths the number of particles in the shower is maximal and the main fraction of energy is deposited. Beyond the shower maximum the central core disappears. This is due to multiple scattering of mainly low energy electrons, their bremsstrahlung and $\gamma$-conversion or Compton scattering which widenes the shower over some Moliere radii. Specially the well located energy core within the first 2 - 3 radiation lengths can be used to precisely determine the location of the incident electron by measuring the center of gravity (cog). This can be achived by not only segmenting the detector in the $x, y - plane$ but also longitudinally in $z - direction$.

As was shown the FMC radial shower profile simulation integrated over the total depth $z$ agreed fairly well with the GEANT simulation. Additionally – for logitudinally segmented electromagnetic detectors – the transverse energy distributions for different depths inside the material have to be correctly simulated by the FMC program. Figs. 20 a, b and c show for 10 GeV electrons in $CeF_3$ a comparison of FMC and GEANT for the radial energy distributions in depths of 10, 20, and 30 cm , respectively. In all cases the agreement is sufficient.

# 5 Energy and Space Resolution

As a test of the FMC the energy and space resolution for a 10 GeV electron was estimated for different detector volumes and compared to GEANT predictions.

The electromagnetic detector consisted of $CeF_3$ and was essentially modified in volume size. With two crystal types ($2 \times 2$ and $3 \times 3$ $cm^2$ front face) and three different matrix-setups ($3 \times 3$, $5 \times 5$, and $7 \times 7$ crystals) a total of six detector volumes could be constructed. All crystals were quaders, 25 $X_0$ long. In fig. 21 the GEANT setup of a $5 \times 5$ crystal matrix is scetched. The simulation is started with a 10 GeV electron hitting the matrix in the middle of the central crystal front face and perpendicular to it.

As noted in ch. 2.4 the number of hits in the FMC can be used to steer the local fluctuations and consequently the energy resolution. For a 10 GeV electron incident on $CeF_3$ the effect of local shower fluctuations is illustrated in figs. 22 a, b and c. Displayed are three individual showers, each created with a different number of hits (500, 5000 and 50000, respectively). One recognizes, that there are – as expected – more local fluctuations, if the number of hits is small. This shows for example, that the energy resolution of a finite detector volume becomes worse, since the deposited energy (i.e. the number of hits inside the detector) decreases and therefore shows stronger fluctuations. We chose the number of hits in such a way, that the energy resolutions simulated by the FMC and by GEANT agreed. The relative energy accuracy $\sigma_E/E$ (energy resolution) was received by simulating 100 times the total energy deposited in the respective detector matrix. $\sigma_E$ was the result of a fit to this energy distribution. 100 simulations of the center of gravity and a fit to the distribution were used to derive the space resolution.

In fig. 23 the energy resolution for different matrix sizes for a 10 GeV electron shower is plotted, as calculated by GEANT and by FMC. The number of hits was optimized for the largest detector volume (i.e. $7 \cdot 3cm = 21cm$). 300 hits/GeV were needed; i.e. 3000 hits for 10 GeV electrons. For both, GEANT and FMC the resolutions become worse by decreasing the size of the detector volume, but the resolutions predicted by GEANT are better than the FMC-resolutions. This shows that in the FMC program the number of hits per GeV has to be tuned carefully to the special detector size.

In fig. 24 the space resolutions for three different matrix sizes is plotted. One recognizes a fair agreement of GEANT and FMC predictions.

# 6 Conclusion

A fast Monte-Carlo program to simulate the energy deposition of electrons in homogeneous electromagnetic calorimeter setups has been developed following a description of a fast Monte-Carlo for a Uran/Scintillator detector from del Peso and Ros [2]. In that report many details of the determination of the parameters are given and the changes necessary for incident photons is described. Fluctuations in the shower development were taken into account by fluctuating the relevant parameters of the longitudinal and radial shower shape functions and the locations of energy deposits. For the most important parameters determining the longitudinal and radial shower shape analytical relations were given, which depend only on the radiation lenght and the Moliere radius of the material. In the FMC the number of hits was tuned to reproduce the energy resolution predicted by GEANT. Longitudinal and integrated radial shower profiles and radial shower profiles as a function of the depth in the material, produced with the FMC, agreed well with GEANT predictions. Furthermore energy and space resolutions predicted by

GEANT could be reproduced with the FMC program. In our studies the FMC was roughly 100 times faster than the GEANT program.

# References


[1] EGS: W. R. Nelson, H. Hirayama, D. O. Rogers, SLAC-265 (1985)
GEANT: R. Brun et al., CERN DD/EE/84-1 (1986)

[2] J. del Peso and E. Ros, DESY-report, DESY 91-005, February 1991

[3] Review of Particle Properties, Phys. Lett. B239 (April 1990) III.15
E. Longo and I. Sestili, Nucl. Instr. and Methods 128 (1985)283

[4] G. Grindhammer, M. Rudowicz, and S. Peters
Nucl. Instr. and Methods A 290 (1990) 469

# List of Figures


1 Parameters $\alpha$ and $\lambda$ for $CeF_3$ and 10 GeV electrons . . . . . .
2 Logarithms of parameters $\alpha$ and $\lambda$ ($CeF_3$, 10 GeV electrons) . . . . . .
3 Energy dependence of the logarithms of the four parameters for $CeF_3$ (the curves show fits) . . . . . .
4 Energy dependence of the logarithms of the four parameters for $CeF_3$ (the curves show parametrizations) . . . . . .
5 Energy dependence of the logarithms of the four parameters for $BaF_2$ (the curves show parametrizations) . . . . . .
6 Energy dependence of the logarithms of the four parameters for $PbF_2$ (the curves show parametrizations) . . . . . .
7 $\alpha_r$ at different shower depths for $CeF_3$, (the line is a fit, the dashed line a parametrization) . . . . . .
8 $\alpha_r$ at different shower depths for $BaF_2$, (the line is a fit, the dashed line a parametrization) . . . . . .
9 Standard Deviations of logarithms of the four parameters for $CeF_3$ as function of energy, (the curves show fits) . . . . . .
10 Longitudinal and integrated radial shower profile for a 10 GeV electron in $CeF_3$. GEANT (histogram) compared to parametrization (line) . . . . . .
11 Longitudinal shower profile, FMC/GEANT comparison for 10 GeV electrons in $CeF_3$ . . . . . .
12 Longitudinal shower profile, FMC/GEANT comparison for 50 GeV electrons in $CeF_3$ . . . . . .
13 Longitudinal shower profile, FMC/GEANT comparison for 10 GeV electrons in $BaF_2$ . . . . . .
14 Longitudinal shower profile, FMC/GEANT comparison for 10 GeV electrons in $PbF_2$ . . . . . .
15 Mean value of shower depth for different energies in $CeF_3$, a FMC/GEANT comparison . . . . . .
16 Radial shower profile, FMC/GEANT comparison for 10 GeV electrons in $CeF_3$ .
17 Radial shower profile, FMC/GEANT comparison for 50 GeV electrons in $CeF_3$ .
18 Radial shower profile, FMC/GEANT comparison for 10 GeV electrons in $BaF_2$ .
19 Radial shower profile, FMC/GEANT comparison for 10 GeV electrons in $PbF_2$ .
20 FMC/GEANT comparison for radial shower profiles in different depths inside $BaF_2$ . . . . . .
21 GEANT setup of the test matrix . . . . . .
22 Effect of number of hits for local shower fluctuations . . . . . .
23 Intrinsic energy resolution of different matrix sizes for a 10 Gev electron shower in $CeF_3$ . . . . . .
24 Space resolution of the x-coordinate for a 10 GeV electron shower in $CeF_3$ . . .

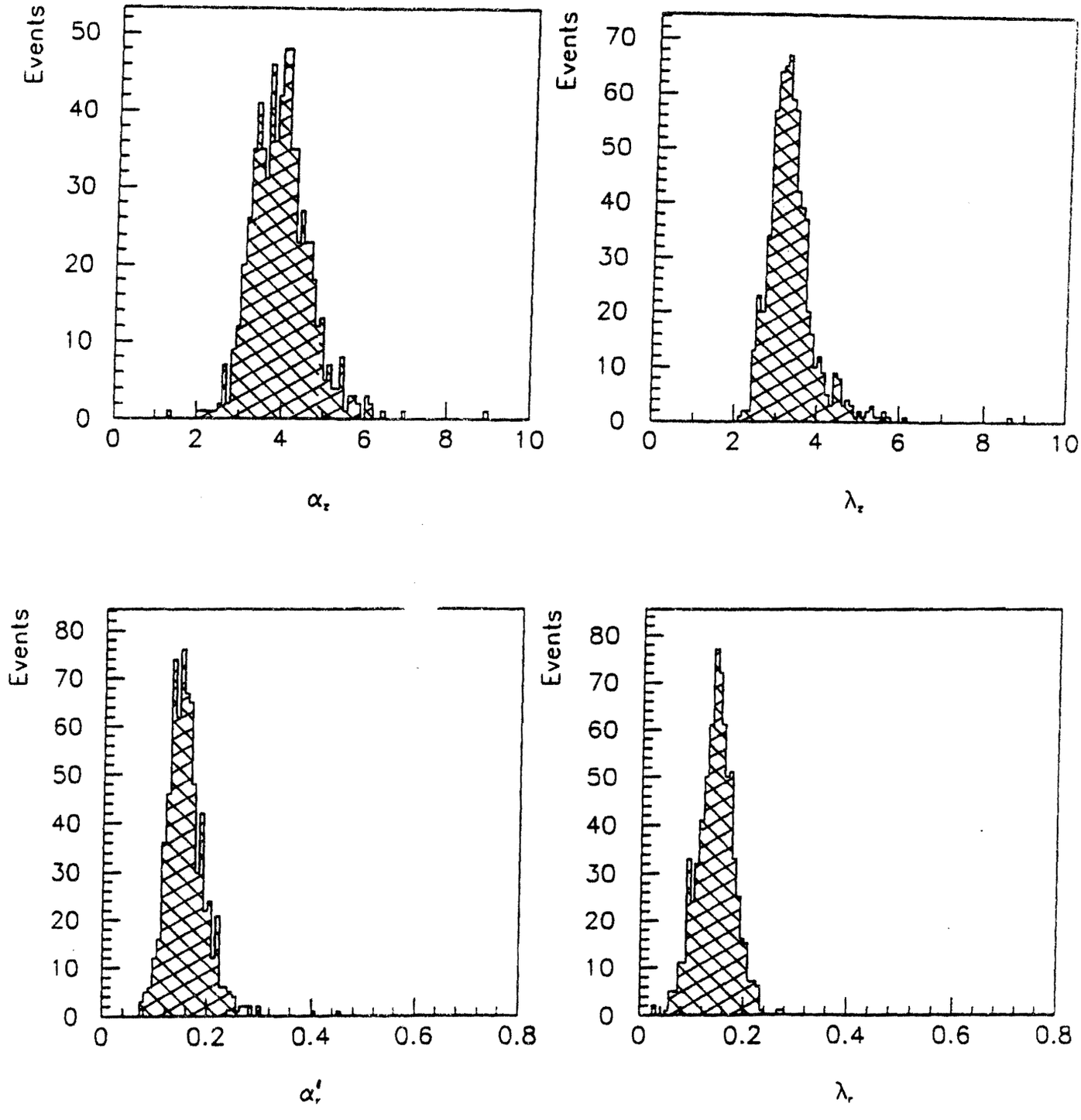


Figure 1: Parameters $\alpha$ and $\lambda$ for $CeF_3$ and 10 GeV electrons

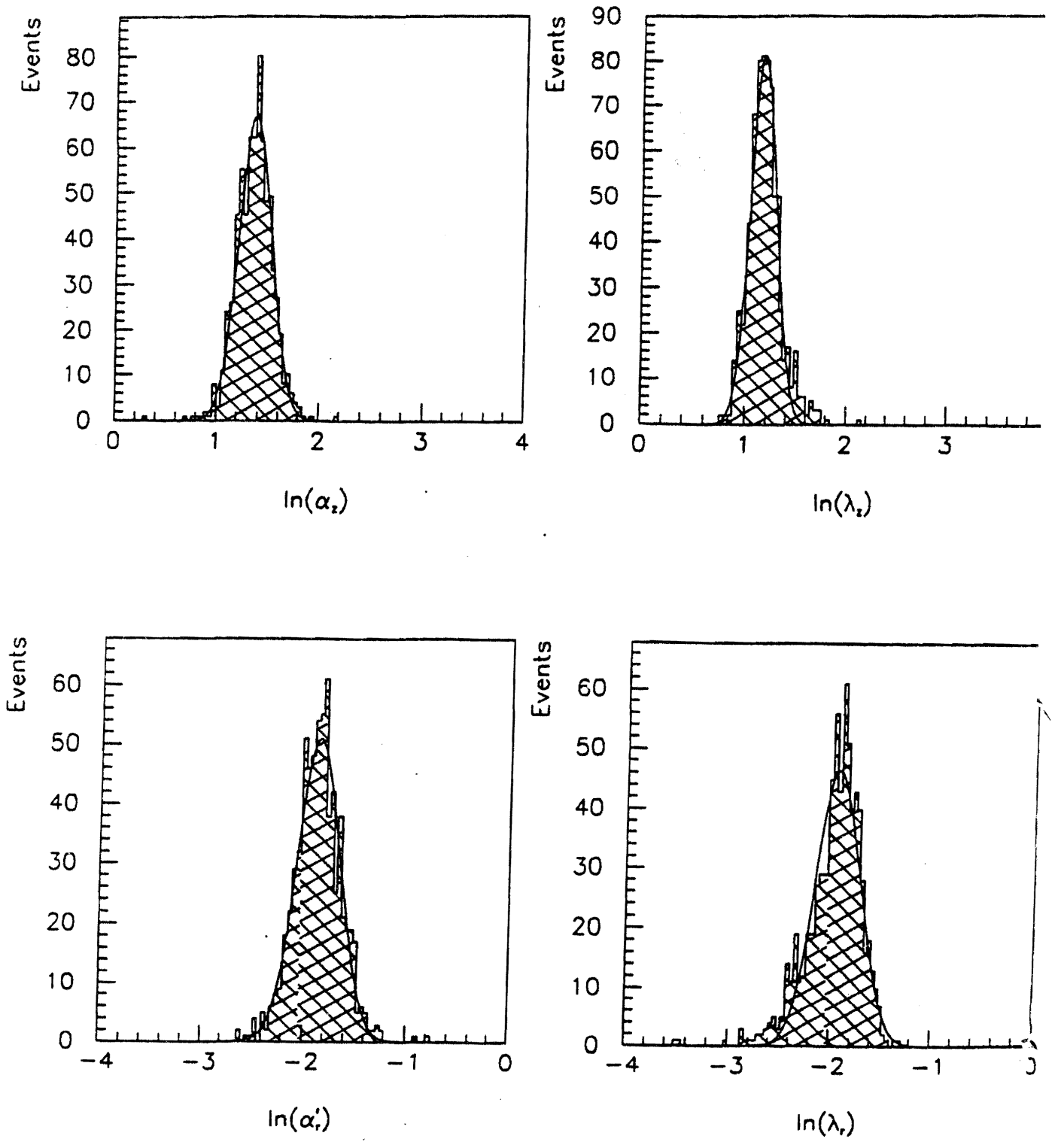


Figure 2: Logarithms of parameters $\alpha$ and $\lambda$ ($CeF_3$, 10 GeV electrons)

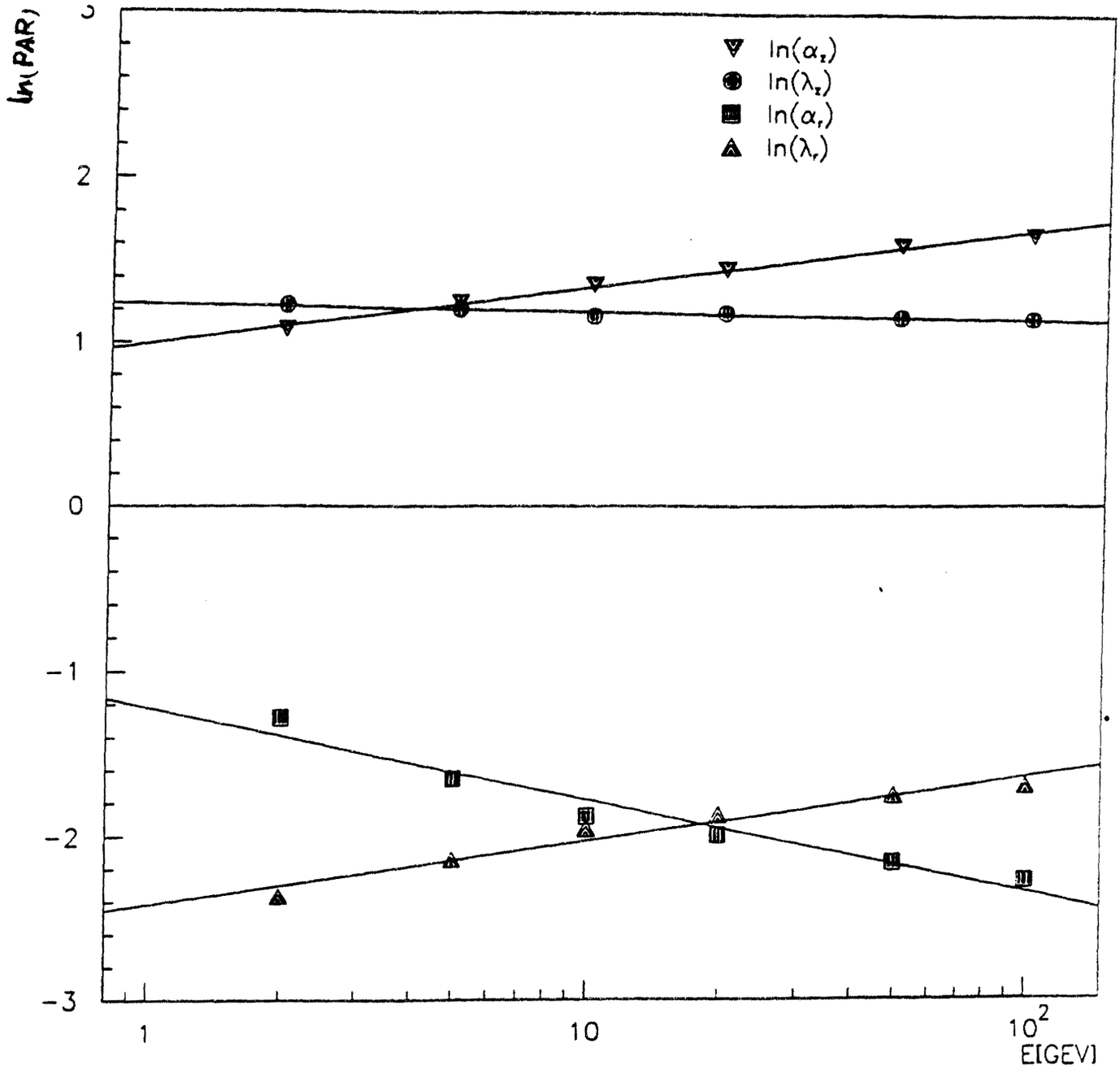


Figure 3: Energy dependence of the logarithms of the four parameters for $CeF_3$ (the curves show fits)

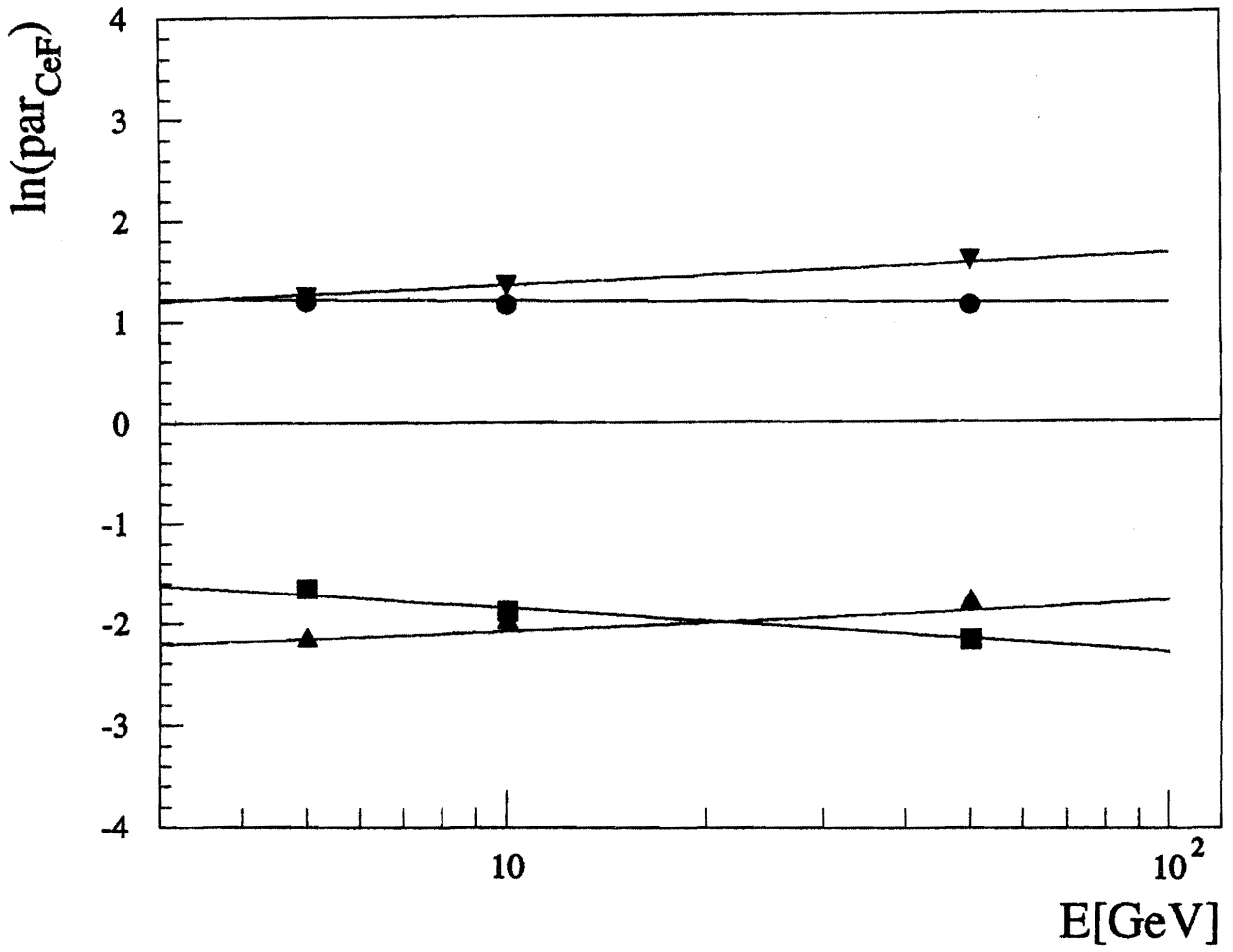


Figure 4: Energy dependence of the logarithms of the four parameters for $CeF_3$ (the curves show parametrizations)

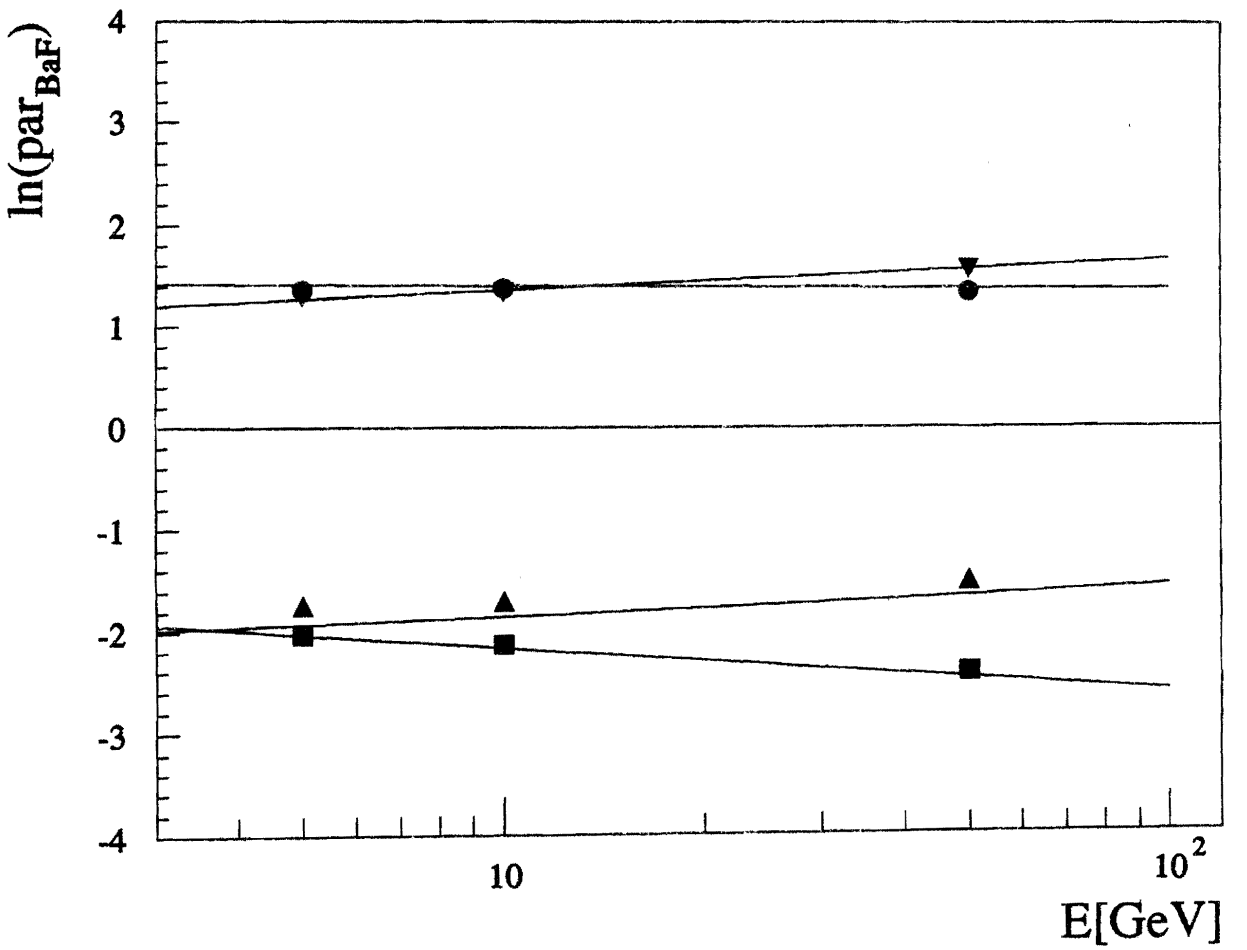


Figure 5: Energy dependence of the logarithms of the four parameters for $BaF_2$ (the curves show parametrizations)

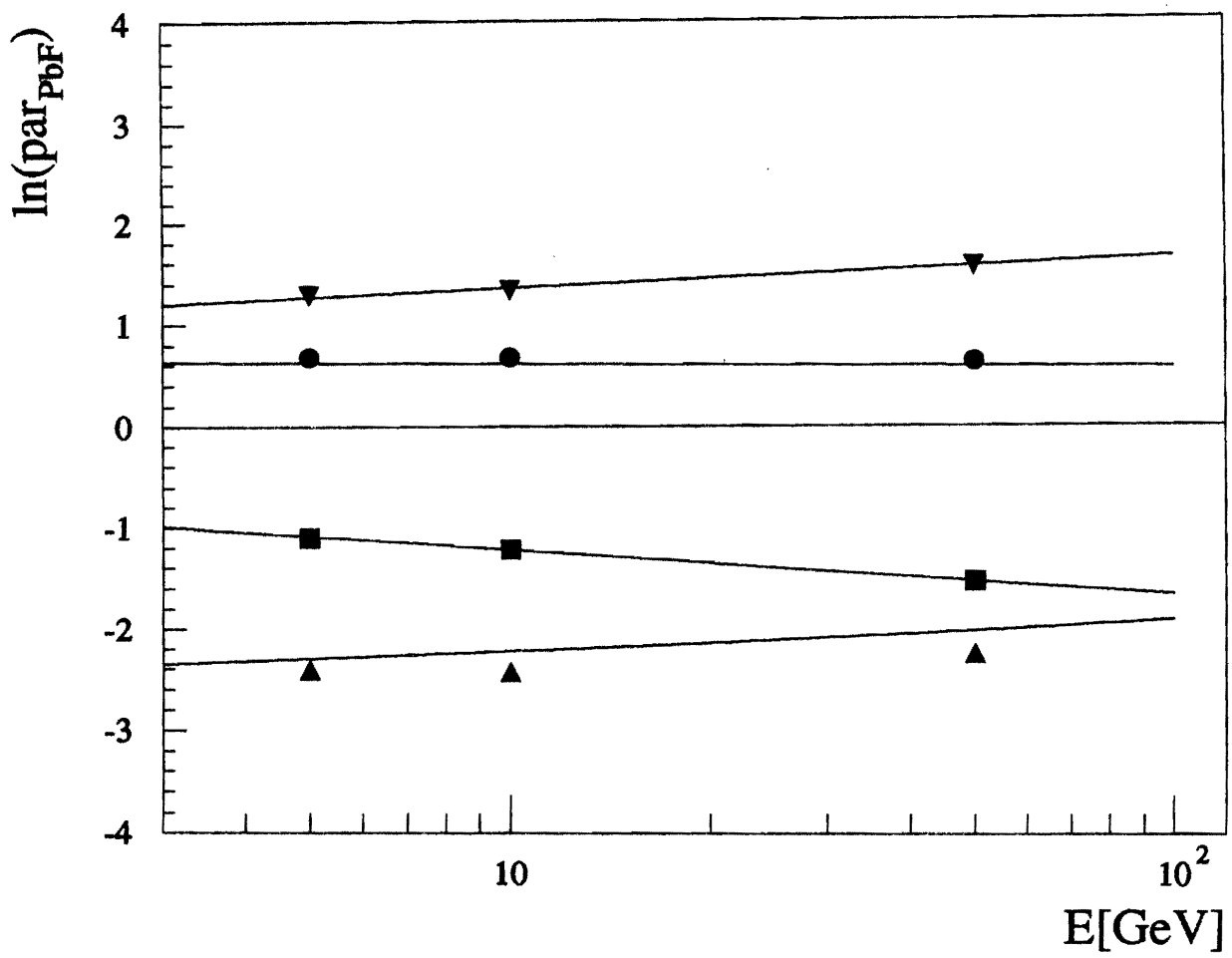


Figure 6: Energy dependence of the logarithms of the four parameters for $PbF_2$ (the curves show parametrizations)

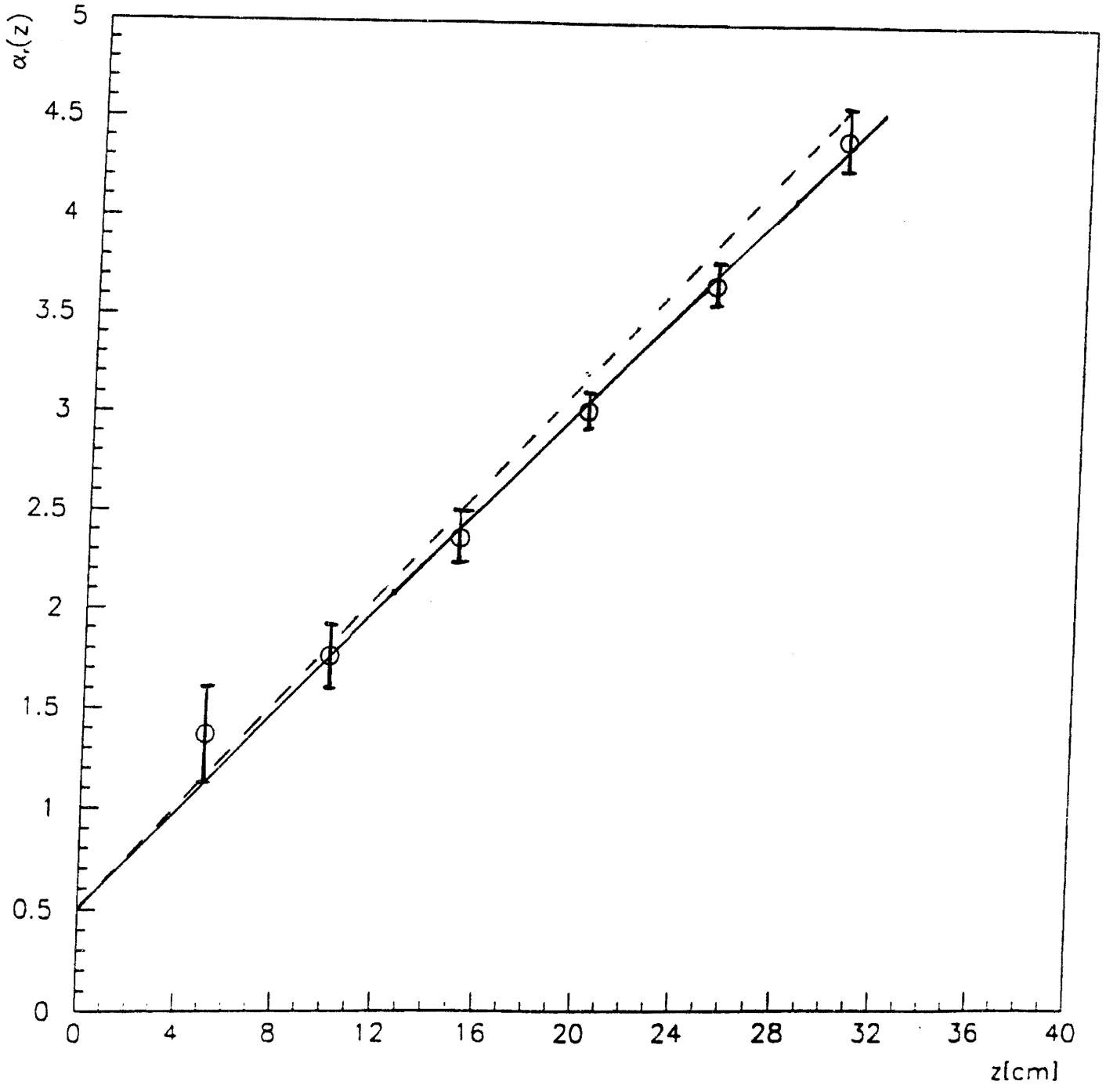


Figure 7: $\alpha_r$ at different shower depths for $CeF_3$, (the line is a fit, the dashed line a parametrization)

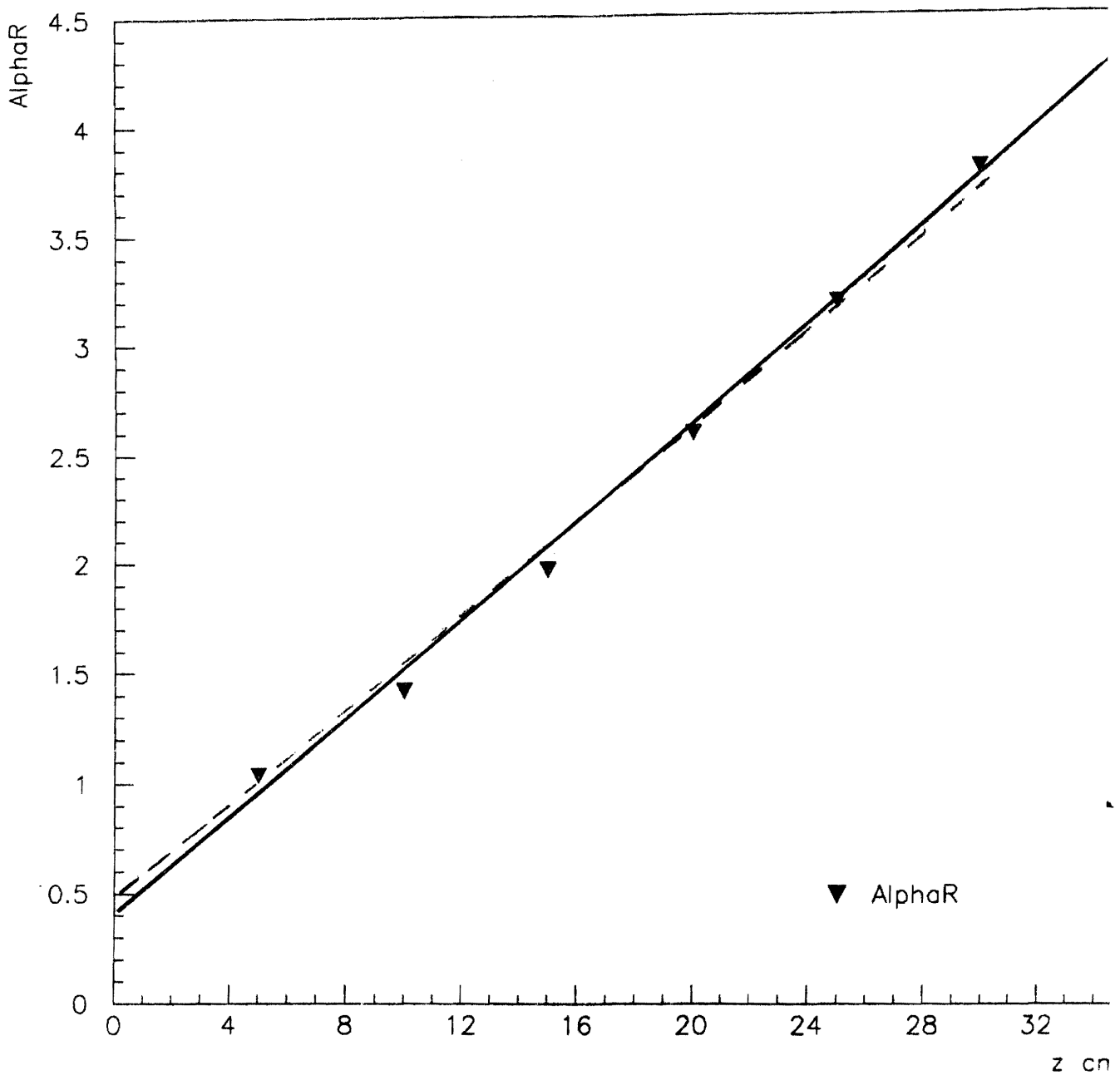


Figure 8: $\alpha_r$ at different shower depths for $BaF_2$, (the line is a fit, the dashed line a parametrization)

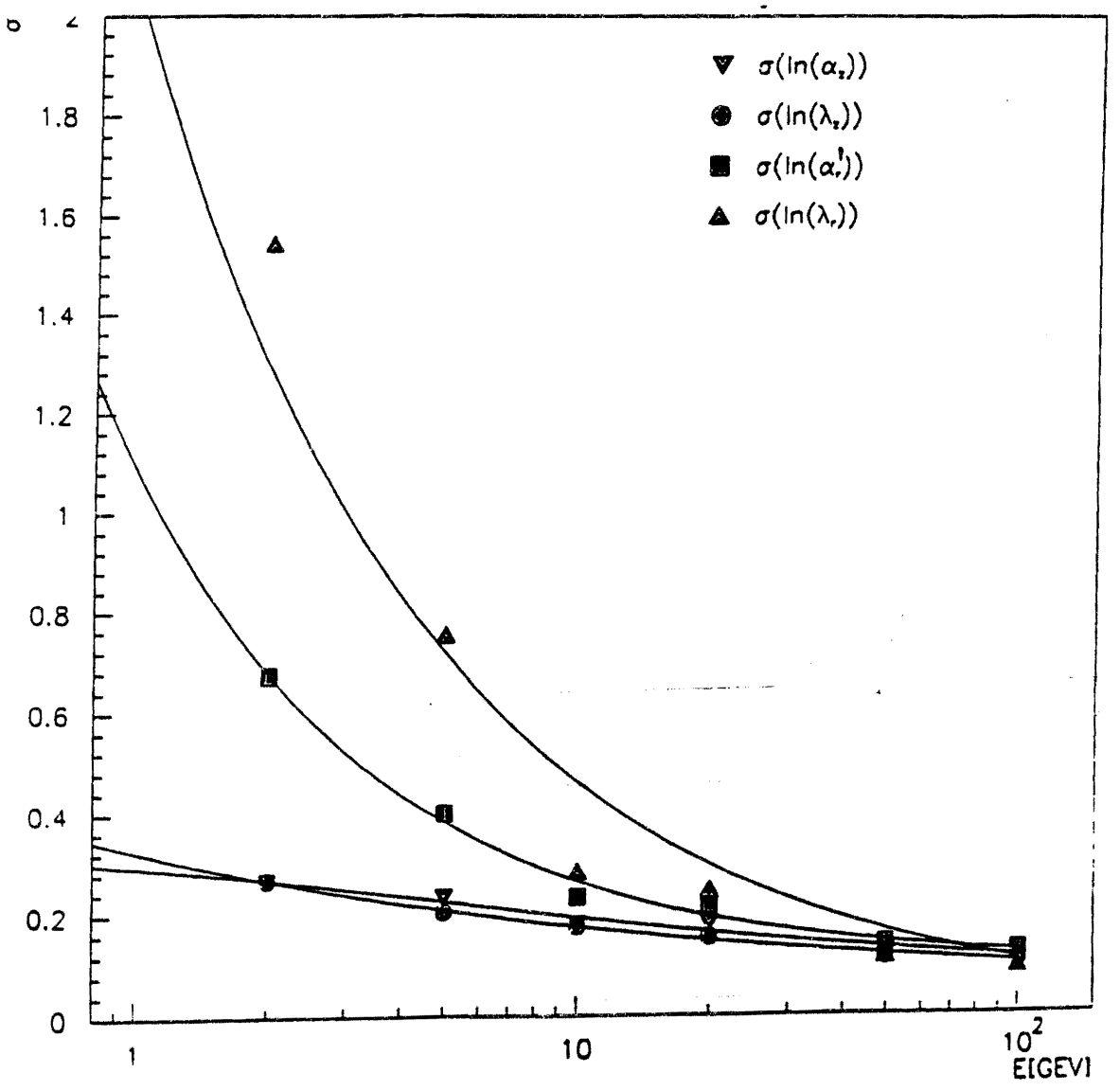


Figure 9: Standard Deviations of logarithms of the four parameters for $CeF_3$ as function of energy, (the curves show fits)

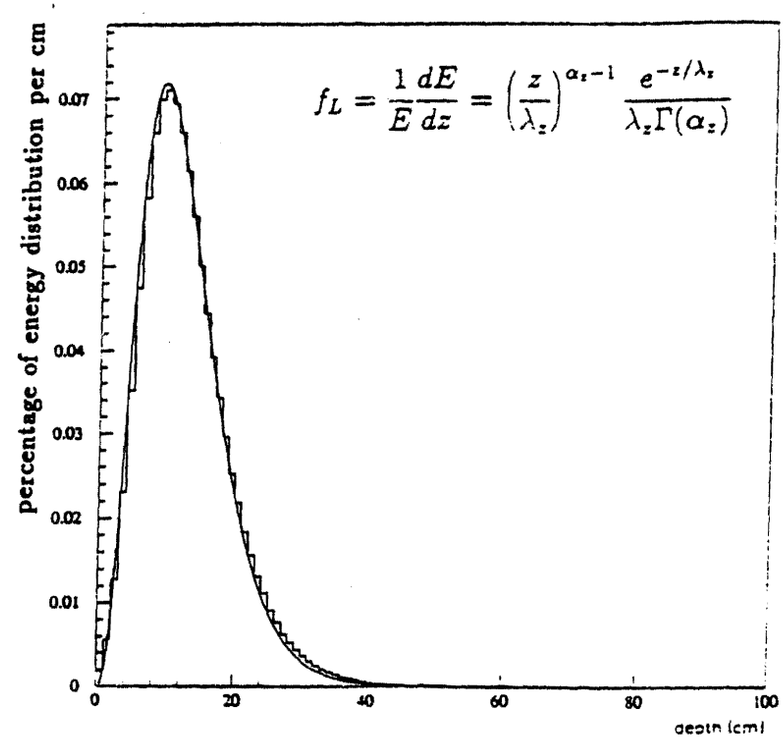


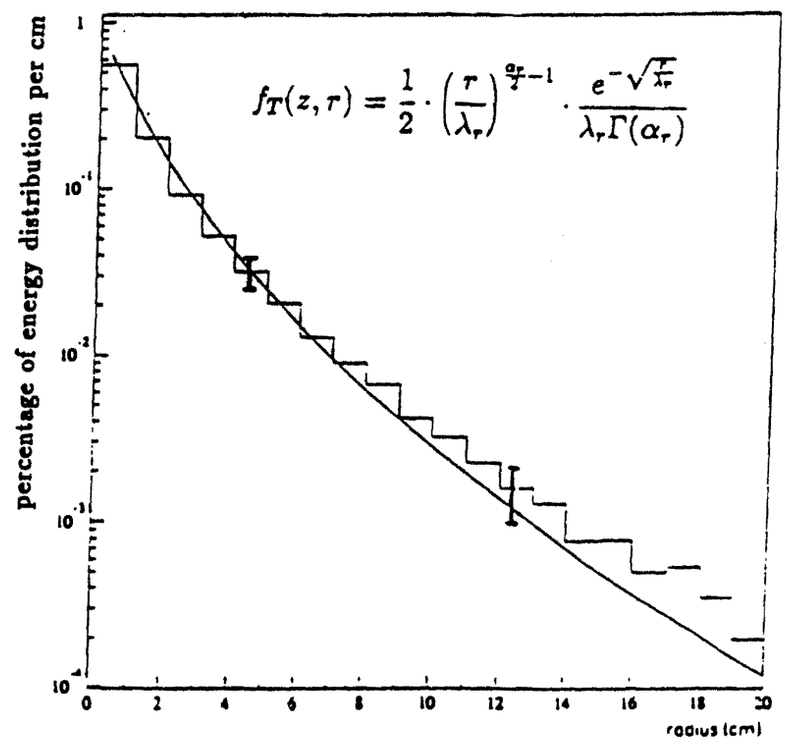


Figure 10: Longitudinal and integrated radial shower profile for a 10 GeV electron in $CeF_3$. GEANT (histogram) compared to parametrization (line)

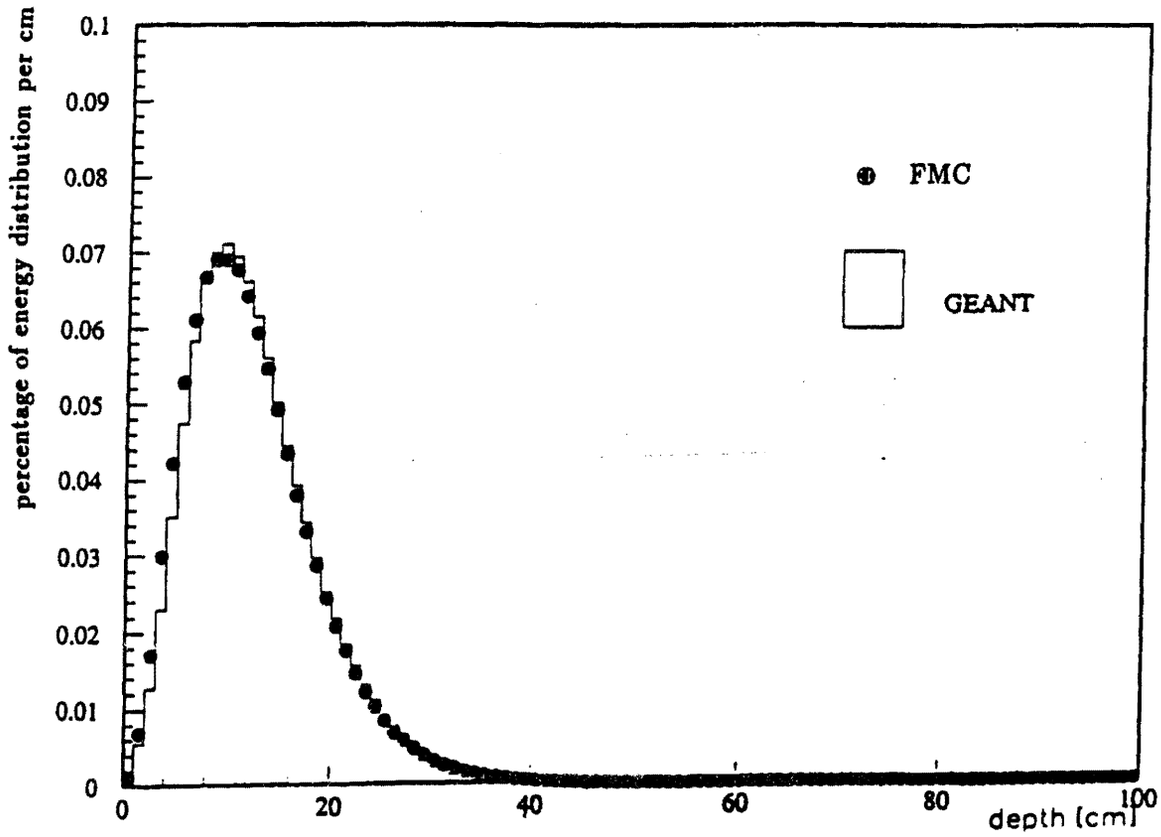


Figure 11: Longitudinal shower profile, FMC/GEANT comparison for 10 GeV electrons in $CeF_3$

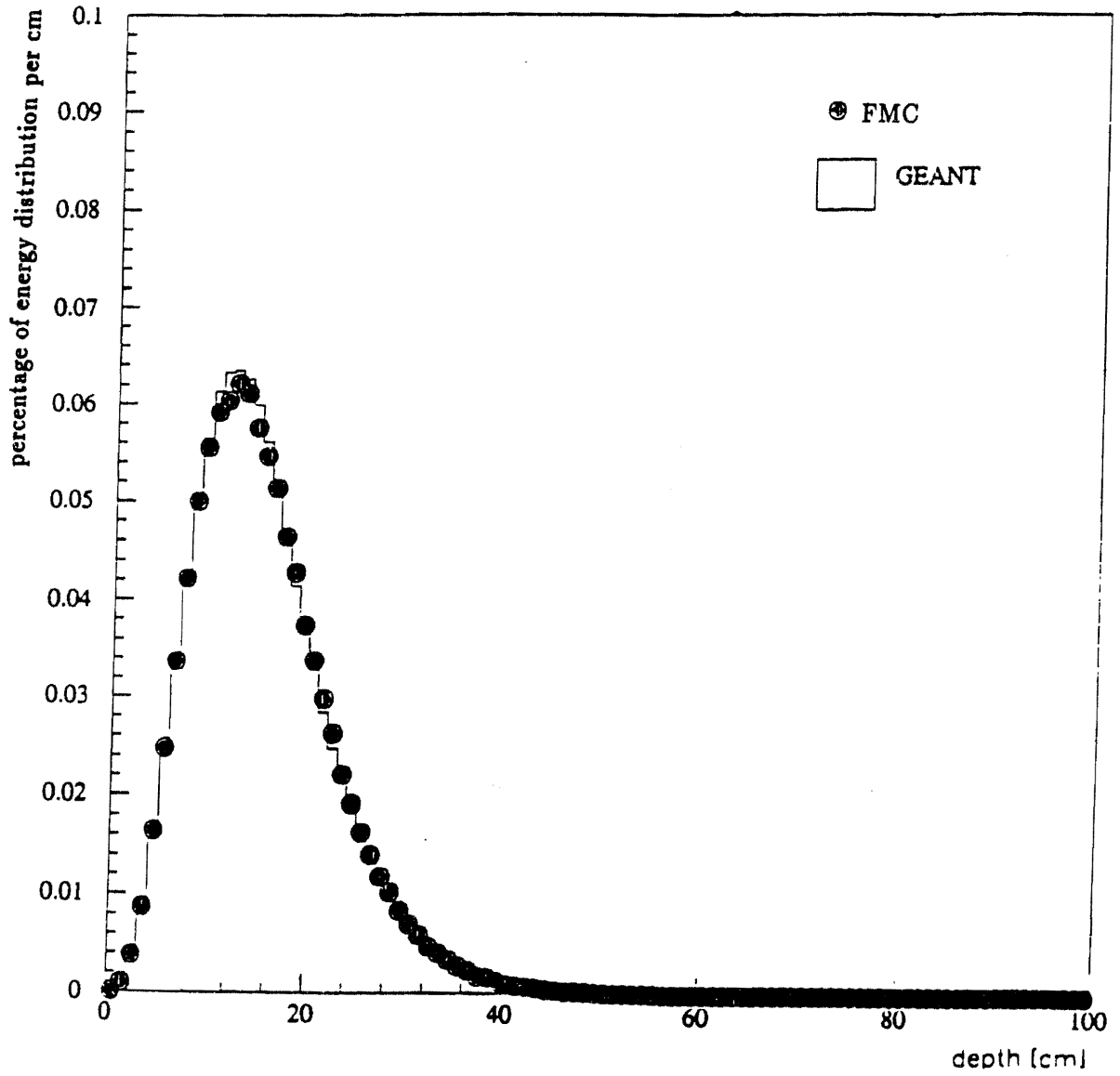


Figure 12: Longitudinal shower profile, FMC/GEANT comparison for 50 GeV electrons in $CeF_3$

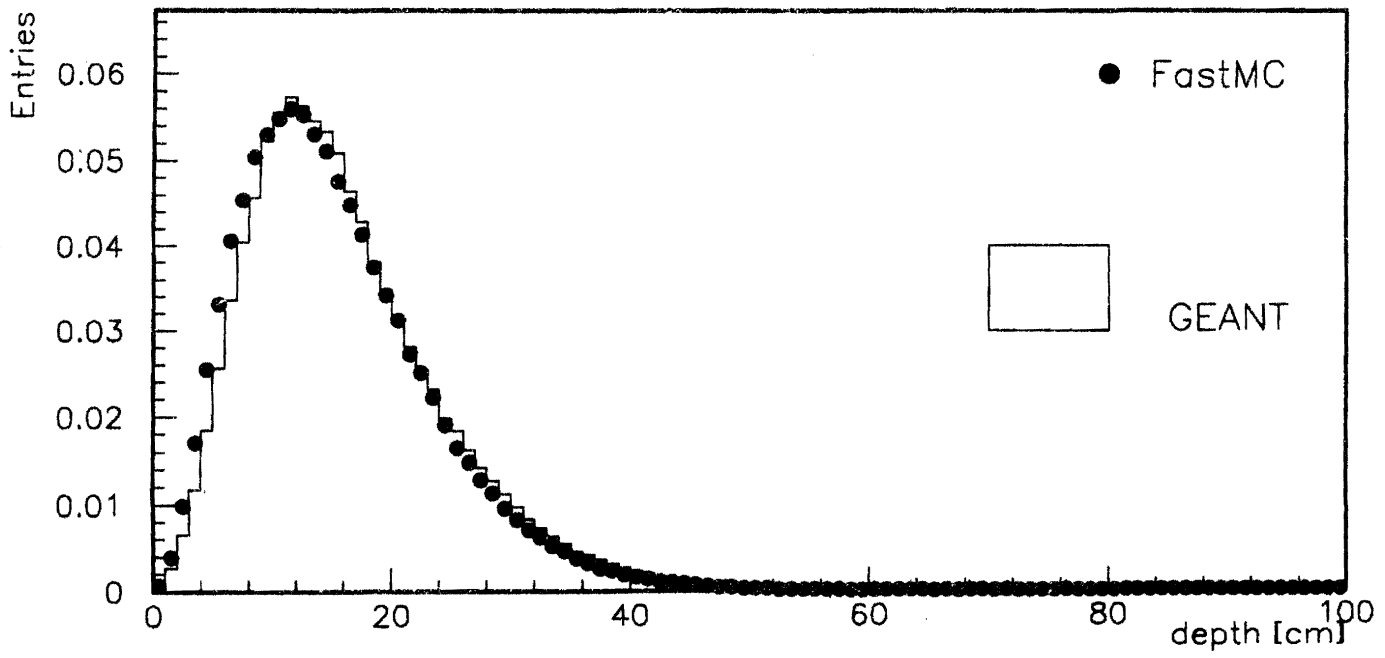


**Figure 13: Longitudinal shower profile, FMC/GEANT comparison for 10 GeV electrons in $BaF_2$**

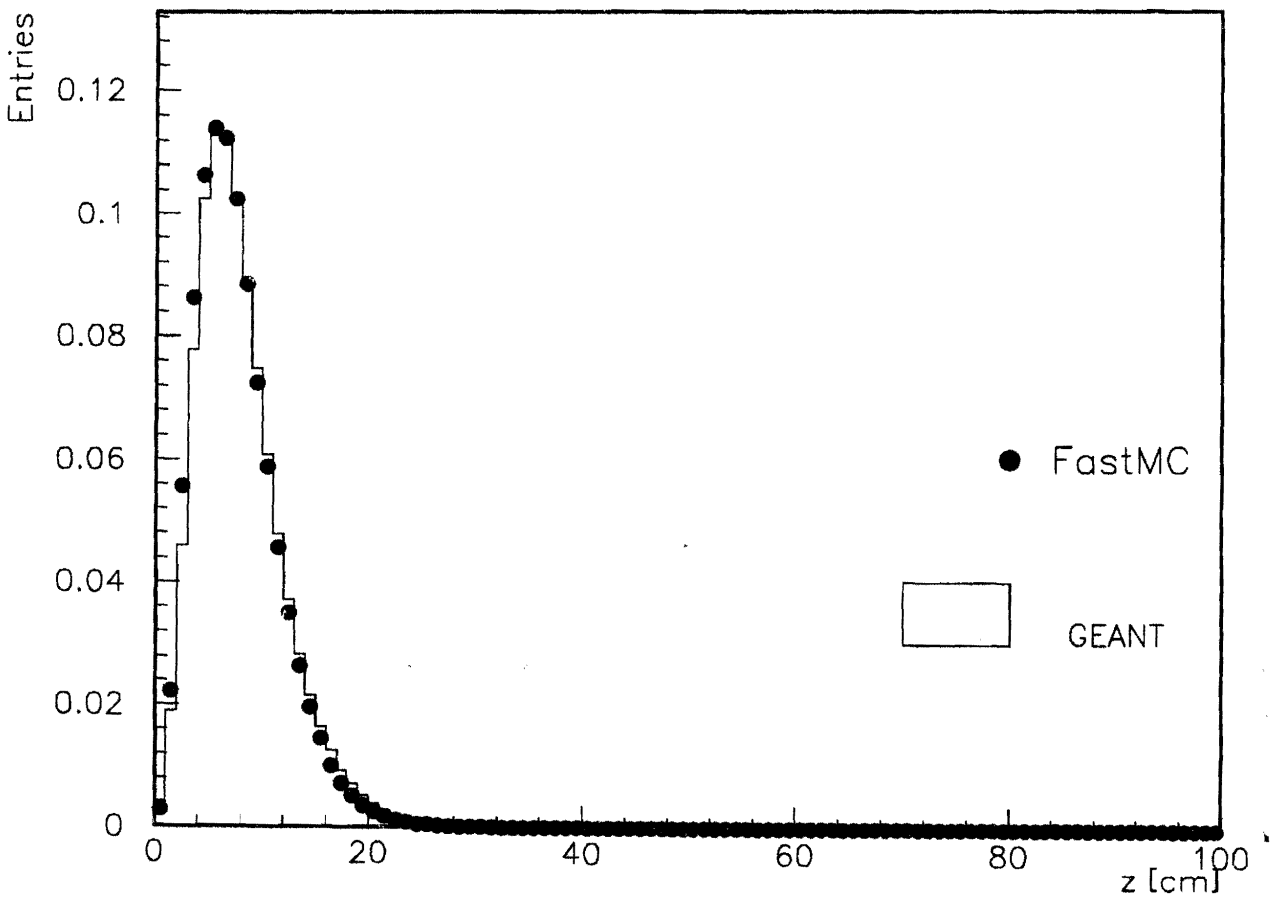


Figure 14: Longitudinal shower profile, FMC/GEANT comparison for 10 GeV electrons in $PbF_2$

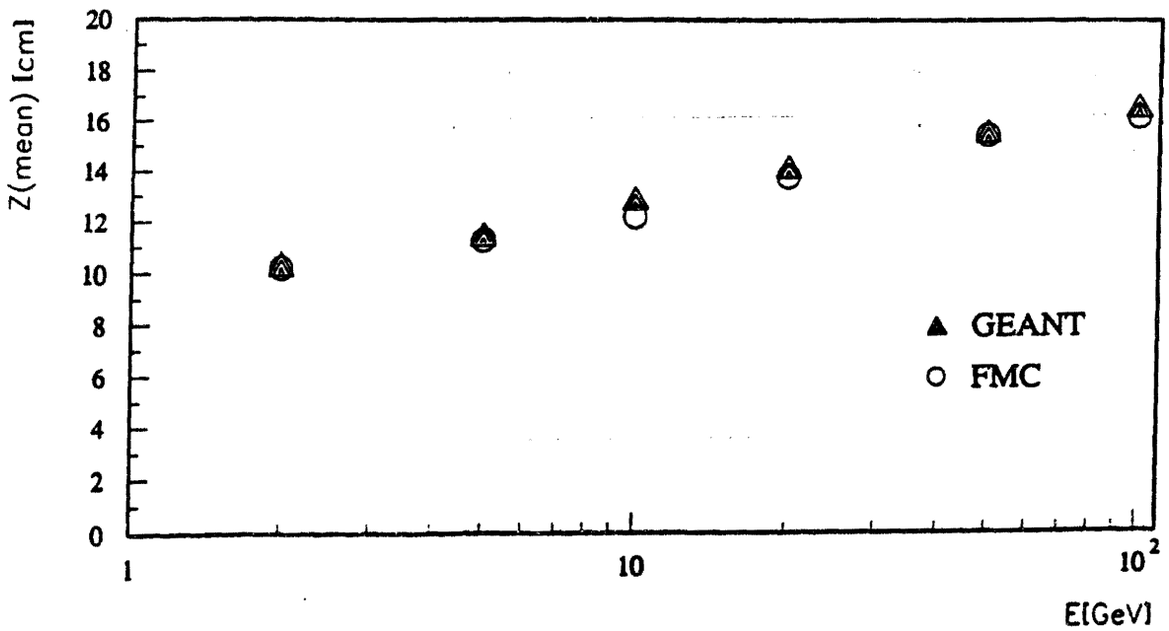


Figure 15: Mean value of shower depth for different energies in $CeF_3$, a FMC/GEANT comparison

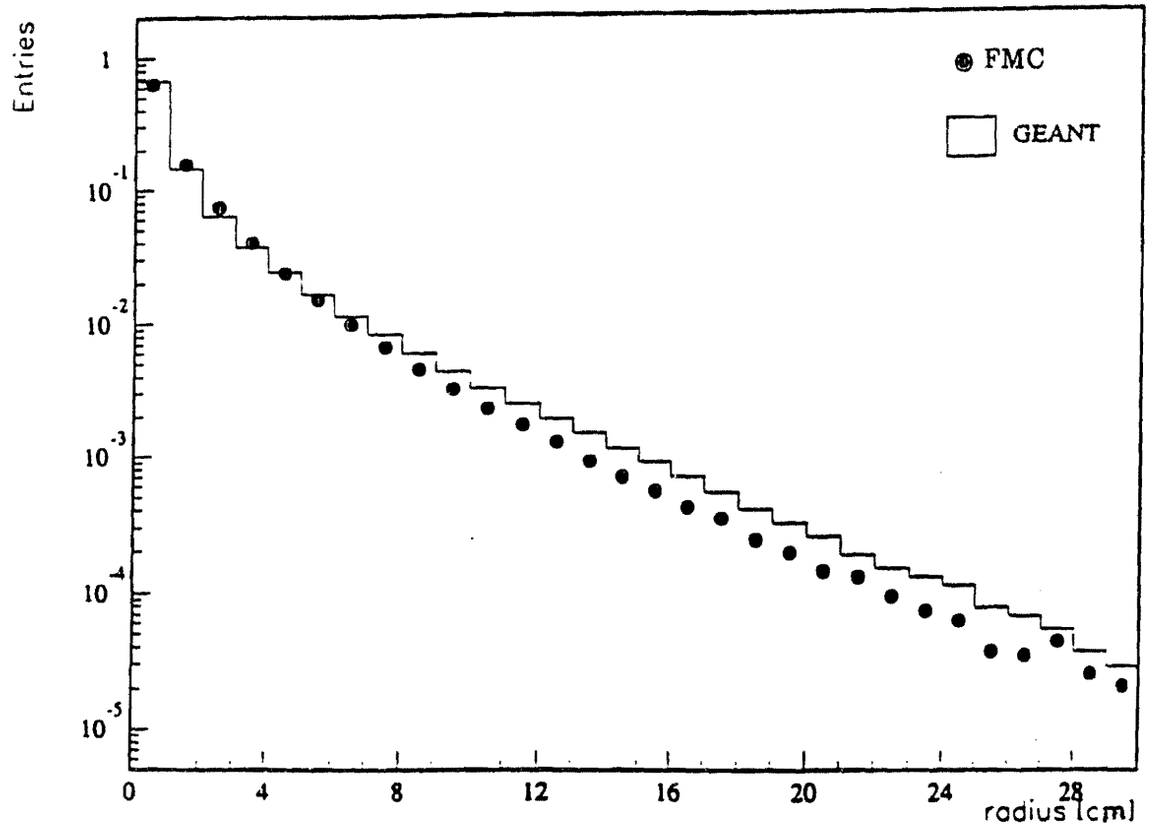


Figure 16: Radial shower profile, FMC/GEANT comparison for 10 GeV electrons in $CeF_3$

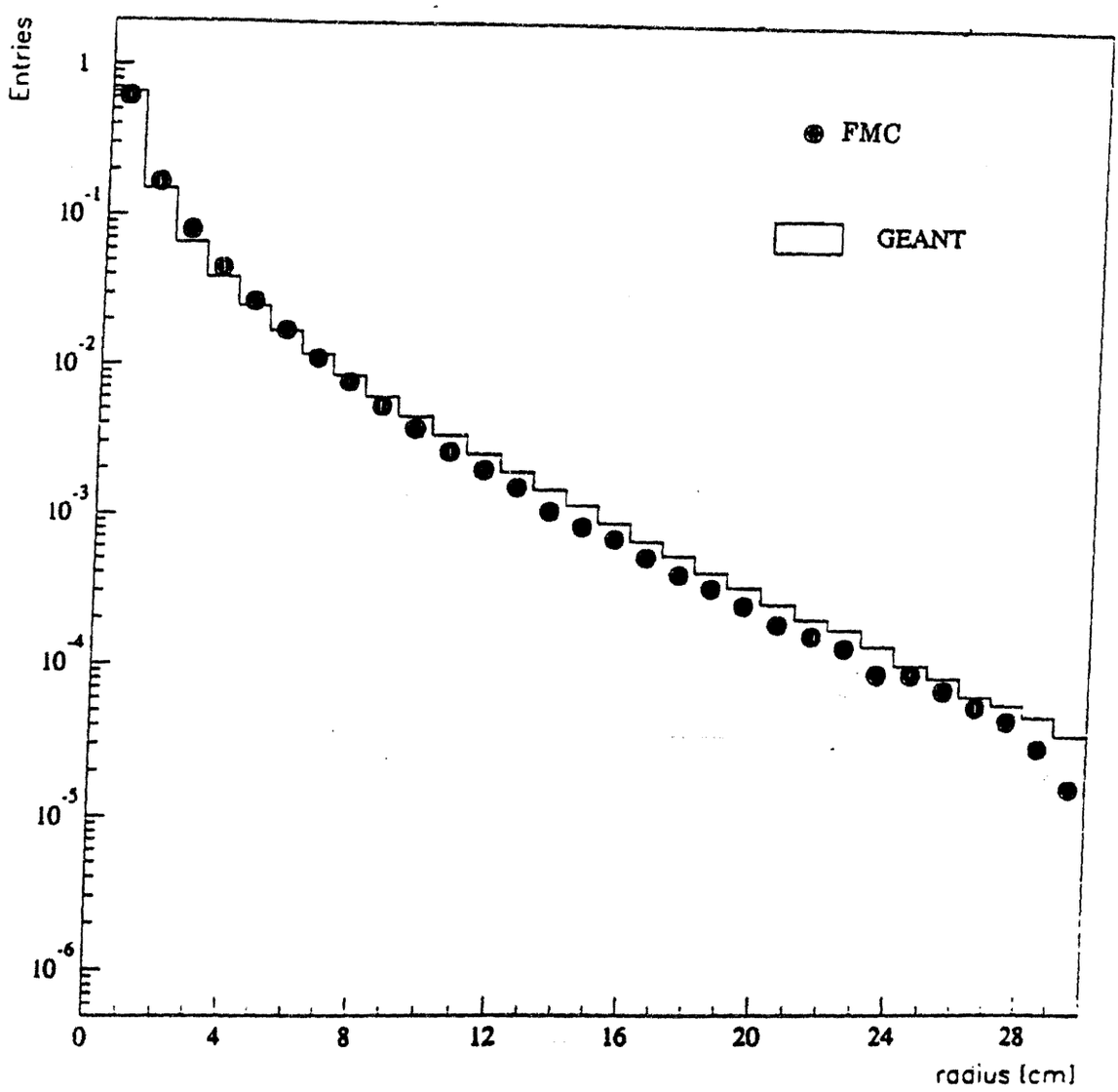


Figure 17: Radial shower profile, FMC/GEANT comparison for 50 GeV electrons in $CeF_3$

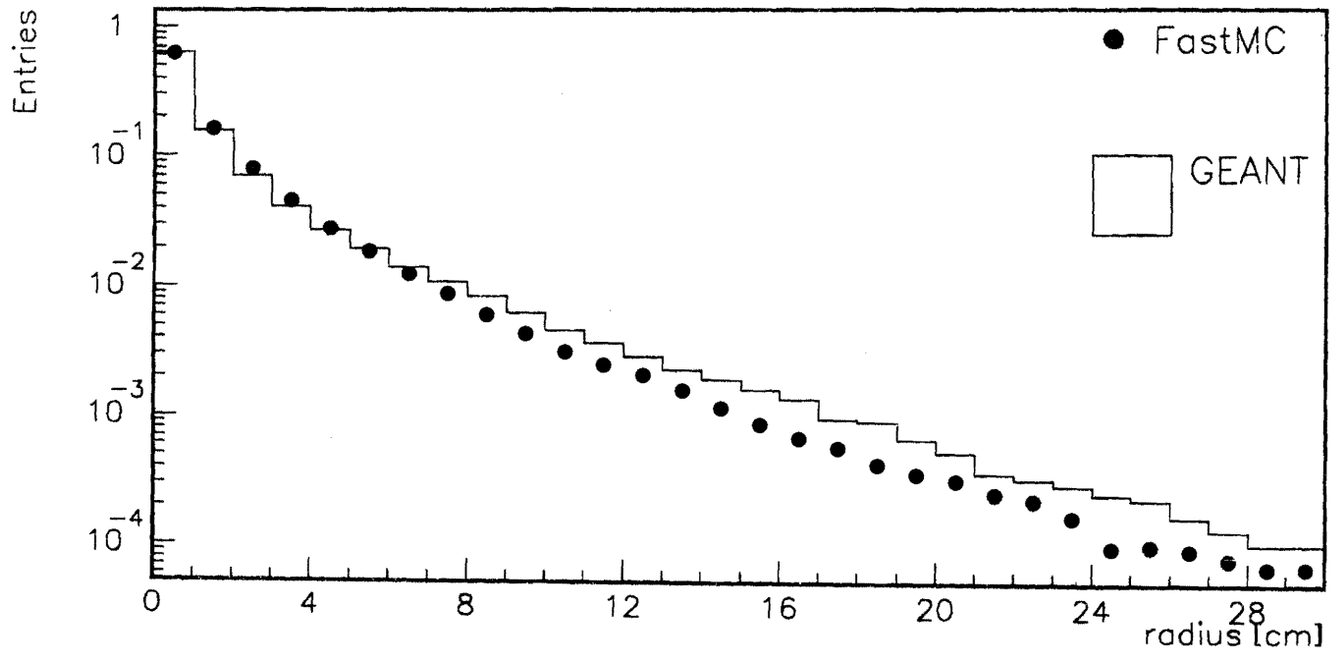


Figure 18: Radial shower profile, FMC/GEANT comparison for 10 GeV electrons in $BaF_2$

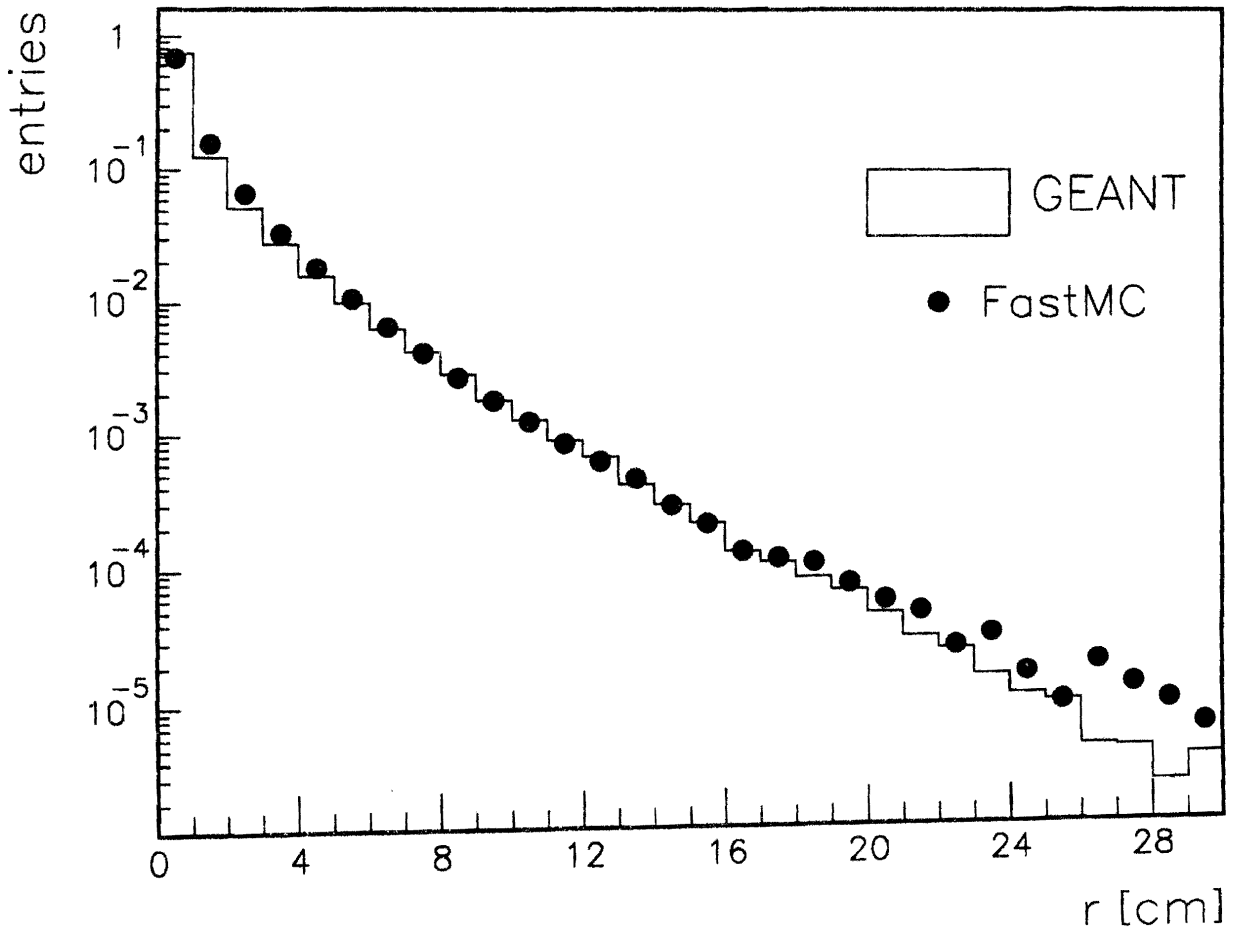


Figure 19: Radial shower profile, FMC/GEANT comparison for 10 GeV electrons in $PbF_2$

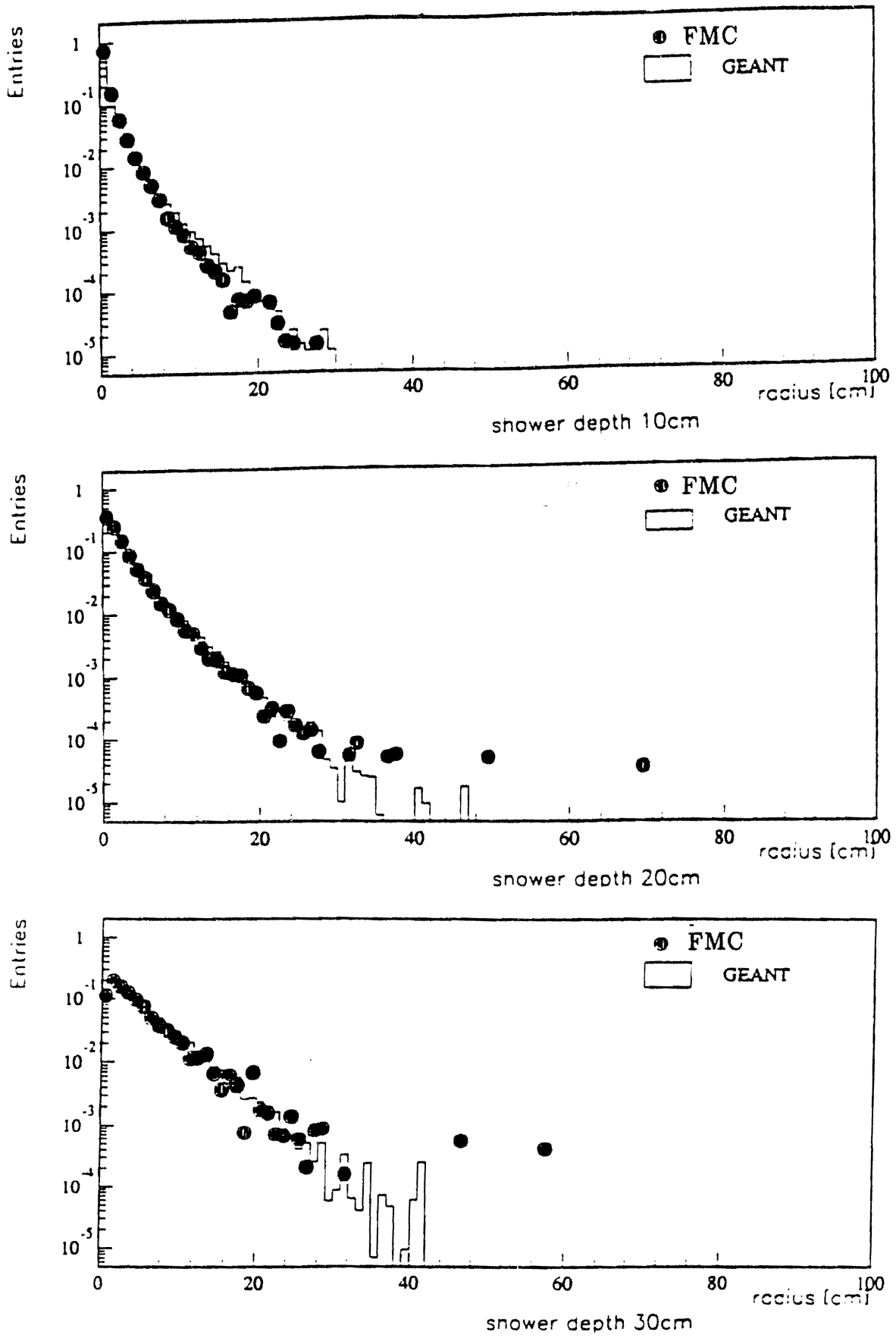


Figure 20: FMC/GEANT comparison for radial shower profiles in different depths inside $BaF_2$

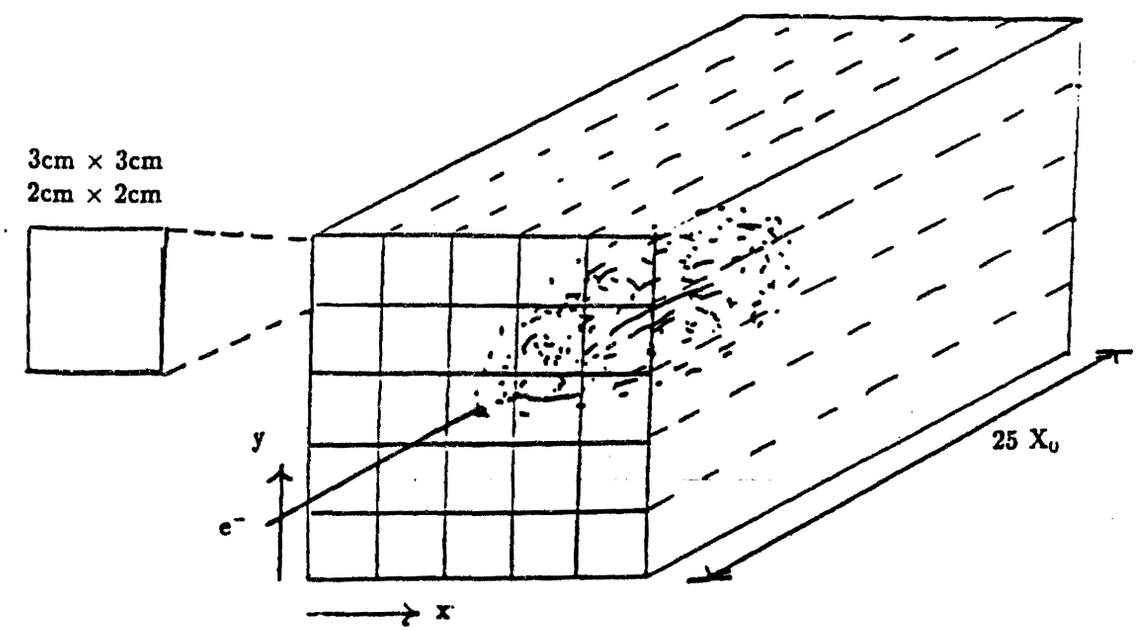


Figure 21: GEANT setup of the test matrix

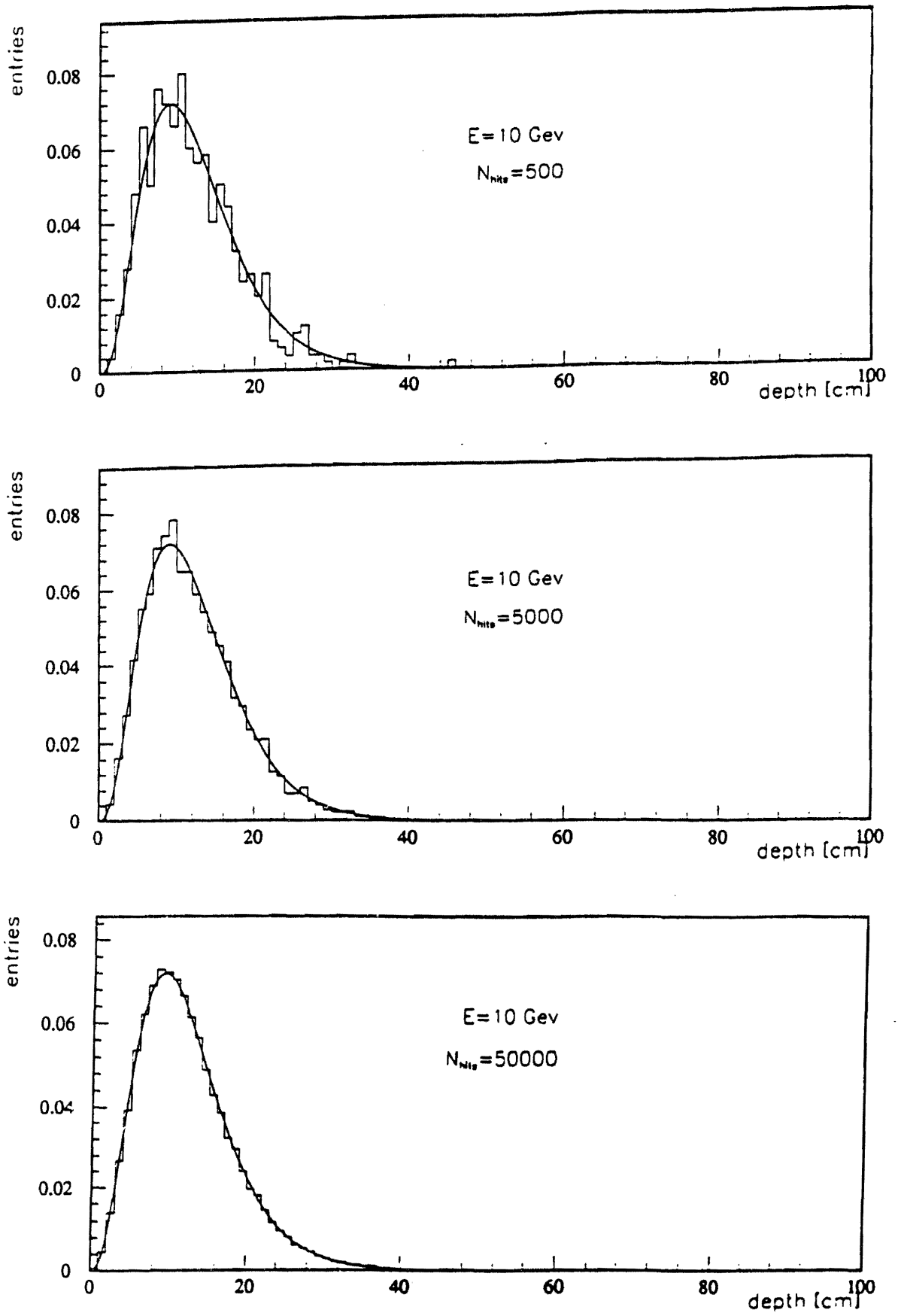


Figure 22: Effect of number of hits for local shower fluctuations

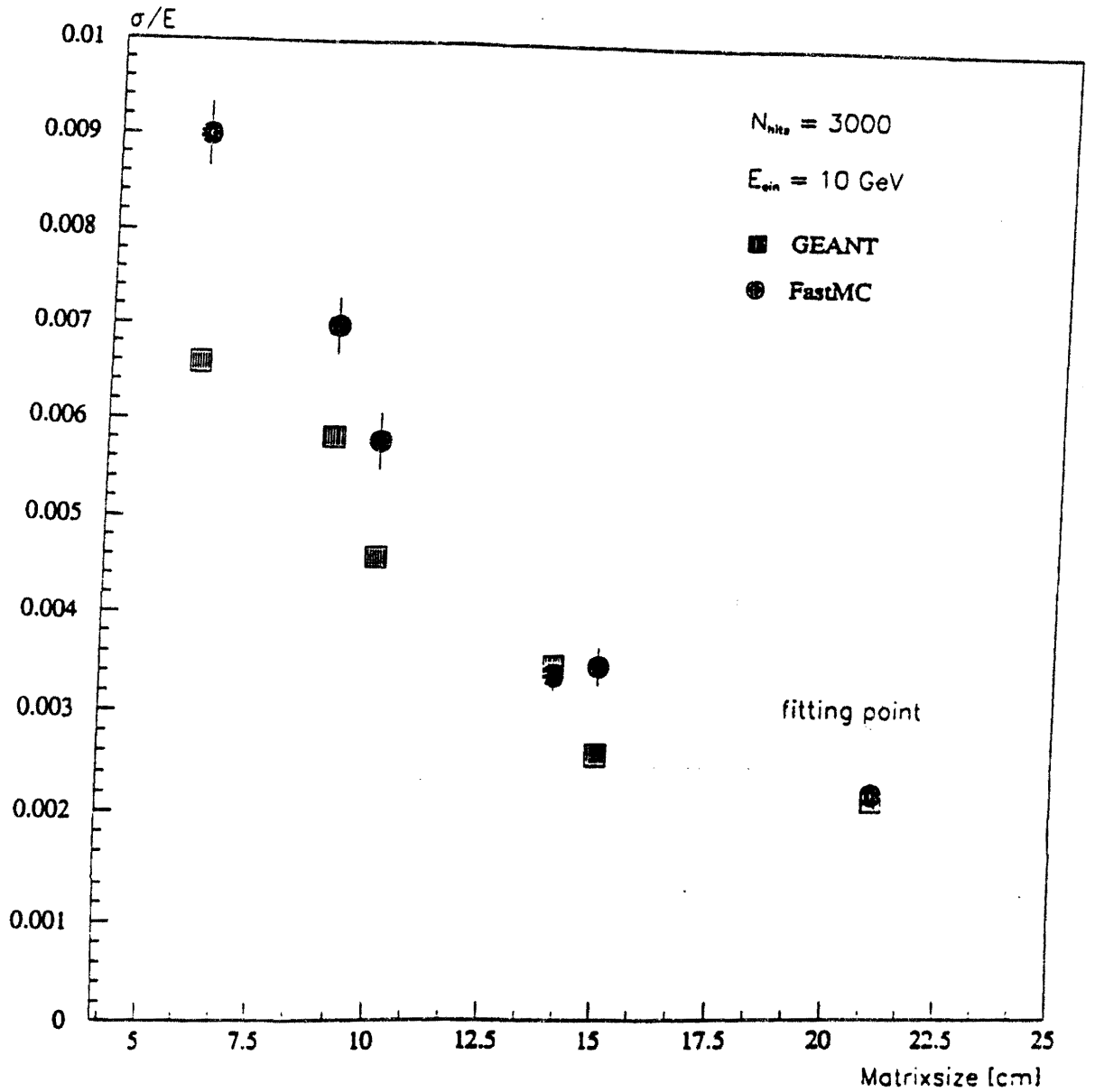


Figure 23: Intrinsic energy resolution of different matrix sizes for a 10 Gev electron shower in $CeF_3$

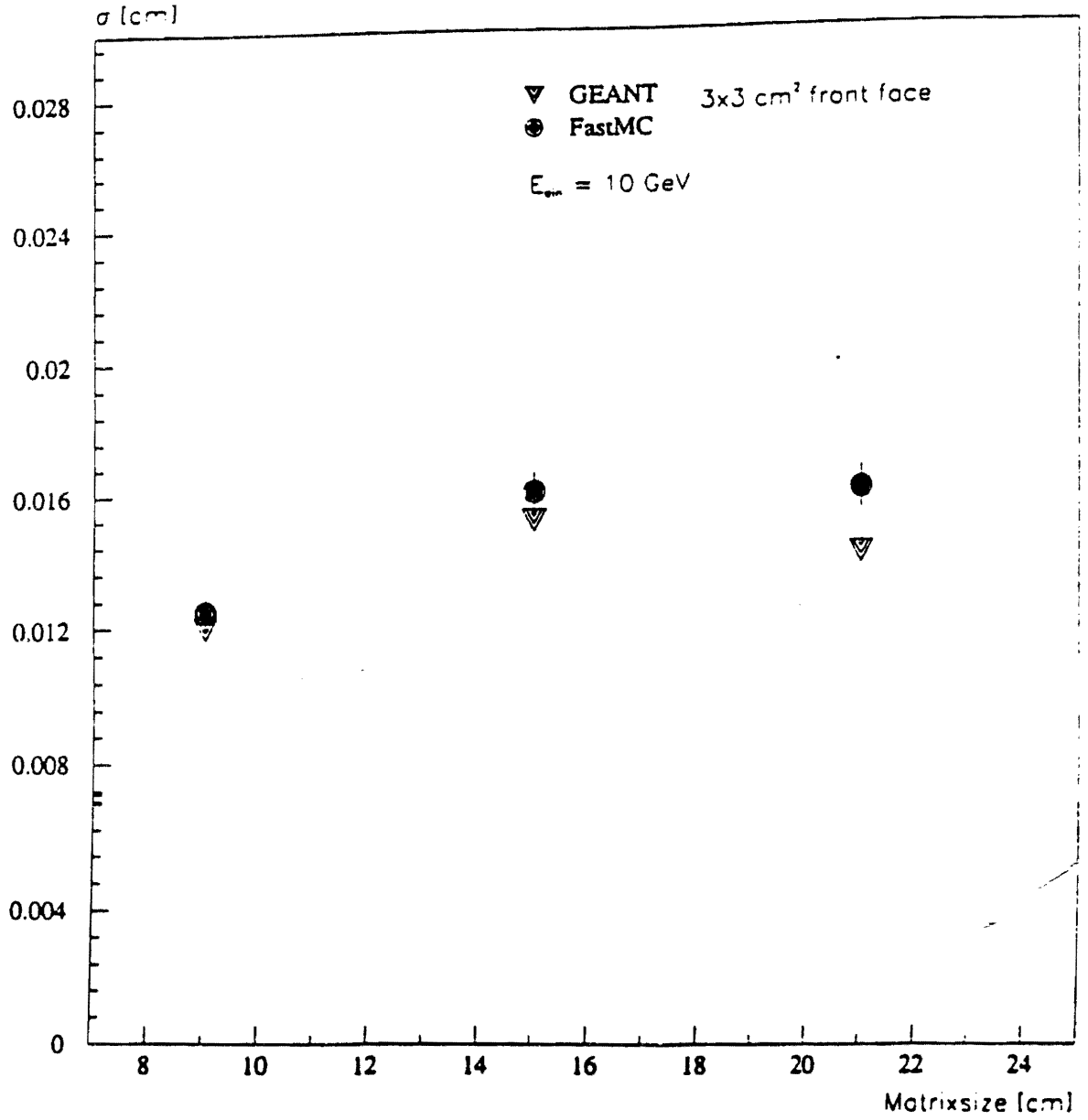


Figure 24: Space resolution of the x-coordinate for a 10 GeV electron shower in $CeF_3$